

Imaging of Nonmalignant Occupational Lung Disease

Jeung Sook Kim, M.D.*† and David A. Lynch, M.B.*

Summary: The radiologist plays an important partnership role in detecting presymptomatic disease in those at risk for occupational lung disease, contributing to the specificity of the diagnosis and recognizing sentinel events. Medicolegal roles for imaging include confirming the presence of a morphologic abnormality compatible with occupational lung disease, identifying other potential causes for disability, and determining the morphologic extent of disease. This article describes and illustrates the imaging appearance of a wide range of occupational lung diseases.

Key Words: Occupational lung disease—Computed tomography.

Diseases of the lung caused by workplace exposures have been recognized for centuries. Despite substantial knowledge about the agents responsible for these diseases and control measures to reduce exposures, tragically these diseases persist throughout the developed and developing worlds (1).

This issue represents a combination of work by clinicians and radiologists whose interests include occupational and environmental pulmonary problems. The radiologist has a key role in the evaluation of miners and foundry or factory workers exposed to mineral dusts and in the evaluation of workers exposed to the “biological” dusts, infectious agents, cancer-causing agents, and chemicals causing interstitial lung disease. The chest radiograph in conjunction with the occupational history, clinical examination, and pulmonary function tests is an important diagnostic tool in the assessment of workers at risk for occupational lung disease. It is also an important monitor of disease progression and one of several criteria used in the assessment of disability. The chest radiograph, however, has a number of limitations, particularly in regard to detection of early disease. In the past decade, computed tomography (CT), particularly high-resolution CT (HRCT), has allowed major improvements in the assessment of occupational lung disease. Although CT has proved to

have greater sensitivity than the chest radiograph, some controversy still remains in regard to the specificity of CT findings in patients suspected of having early pneumoconiosis or hypersensitivity pneumonitis (2).

PNEUMOCONIOSIS

Silicosis/Coal Worker’s Pneumoconiosis

Silicosis is a chronic fibrosing disease of the lung produced by prolonged and/or intense exposure to free crystalline silica. The inhalation of coalmine dust may lead to the development of coal worker’s pneumoconiosis (CWP) and silicosis. Although silicosis is the most common pneumoconiosis, CWP is more common in coal miners (3,4).

Coal mine dust inhaled by miners and other coal workers predispose them to chronic bronchitis, simple pneumoconiosis, focal emphysema, complicated pneumoconiosis (progressive massive fibrosis [PMF]), and mycobacterial pulmonary infection. The risk for simple and complicated pneumoconiosis in coal workers increases with the cumulative exposure to coal mine dust and with the rank (carbon content) of the coal (5). Because coal contains a variable proportion of quartz, it has often been difficult to separate the pulmonary effects of coal dust from those of silica. In general, coals of high rank (high carbon content) such as anthracite are associated with higher incidence of CWP. The prevalence of CWP has decreased significantly since 1970, with the introduction of federal mandates to reduce dust levels (6).

Inhalation of silica dust occurs in a wide range of occupations, including most types of mining, tunneling,

*The Department of Radiology, University of Colorado Health Sciences Center, Denver, CO and †The Department of Radiology, College of Medicine, Pochon CHA University, Kyunggi-do, Korea.

Address correspondence and reprint requests to Dr. David A. Lynch, Department of Radiology, University of Colorado Health Sciences Center, 4200 East 9th Avenue, Box A030, Denver, CO 80220. E-mail: david.lynych@uchsc.edu

quarrying, sandblasting, foundry work, and ceramics manufacture. Silica causes four distinct clinical patterns of lung disease: acute silicoproteinosis, accelerated silicosis, simple chronic nodular silicosis, and complicated chronic nodular silicosis. Acute silicoproteinosis is a pulmonary response to massive inhalation of silica (e.g., in sandblasting), which resembles pulmonary alveolar proteinosis radiologically and pathologically. In accelerated silicosis, inhalation of high concentrations of silica over a period of as little as 5 years results in progressive upper lobe nodularity and massive fibrosis, with associated respiratory insufficiency. Simple or chronic nodular silicosis is the most common manifestation, usually developing after 10 to 50 years of lower-level silica exposure.

Silica inhalation predisposes to mycobacterial infection, including *Mycobacterium tuberculosis*, *Mycobacterium kansasii*, and *Mycobacterium avium* complex. This predisposition is probably related to the toxic effect of silica on alveolar macrophages. The risk for tuberculosis (pulmonary and extrapulmonary) is increased three-fold in patients with chronic silicosis (7). More recently, silica has been recognized as a cause of industrial bronchitis, emphysema, and lung cancer in excess of that expected from cigarette smoking alone.

Although the lesions of CWP may be difficult to distinguish radiologically from silicosis, they are clearly distinct pathologically. In coal workers, carbon dust tends to deposit around the respiratory bronchiole, forming a densely pigmented macule with some adjacent fibrosis and focal emphysema. The characteristic silicotic nodule also occurs around the respiratory bronchiole but differs from the coal macule in that there is abundant central fibrosis with hyalinized collagen. The pulmonary arteries may also become involved in the silicotic lesion. Both conditions can progress to PMF, though this is less common in CWP than in silicosis pneumoconiosis. In CWP, progression to PMF may be related to the silica content of the inhaled dust particles.

Workers with simple CWP may have few clinical signs and symptoms and little measurable physiologic abnormality in early stages. The risk for complicated pneumoconiosis increases with higher radiographic category of simple CWP; thus, opportunities to prevent further exposure in miners with disease found on early radiographs should not be missed.

Chronic nodular silicosis is often first recognized radiographically rather than by symptoms or physiologic abnormality. Exertional dyspnea is the earliest symptom of silicosis and is usually of subtle onset and slow progression. Cough and sputum production are common. Chest auscultation is frequently normal in simple silicosis, and digital clubbing is rare. Pulmonary function is

often normal in early disease as well, but a mixed pattern of obstruction and restriction can occur in workers with more advanced disease.

Progressive massive fibrosis from either silicosis or CWP is associated with severe restriction, decreased diffusion capacity, and hypoxemia, with disabling dyspnea being the most common symptom. Accelerated silicosis, associated with high levels of dust exposure, is a more rapidly progressive form of simple silicosis. Acute silicoproteinosis from intense silica exposure presents with rapidly progressive dyspnea and is often fatal.

Proven effective therapy for silicosis and CWP is lacking. Prevention rather than treatment remains the most important approach to reducing silicosis and CWP. Patients who have simple silicosis should be removed from further exposure to minimize risk for disease progression and complications such as mycobacterial infection. The lack of effective treatment emphasizes the role of the radiologist in detecting these pneumoconiosis.

The radiographic and CT features of CWP and silicosis are nearly identical. Chest radiographic findings are multiple, small, round opacities. The nodules are usually well circumscribed, round, and fairly uniform in size and density. Although profusion can be fairly even throughout both lungs, there is commonly upper lobe predominance. The nodules also tend to involve mainly the posterior portion of the lungs (8) (Fig. 1). Calcification of nodules is evident on the radiograph in 10% to 20% of cases (3). In later stages of pneumoconiosis they tend to coalesce and form conglomerate mass-like opacities (PMF) (9). Hilar and mediastinal lymph nodes tend to enlarge and calcify in an eggshell pattern (10,11) (Fig. 2). Radiologically, the only difference between simple CWP and simple silicosis is that the nodules in CWP are often smaller (typically *p* rather than *q* opacities, according to the ILO classification).

The CT findings are sharply defined small nodules that may be diffuse throughout the lungs but frequently are most numerous in the upper lung zones (8) (Fig. 1). These vary with the size of the opacities seen on the chest radiograph. Opacities classified as type *p* by the ILO criteria are characterized on HRCT by tiny branching structures or a cluster of small dots. Centrilobular emphysema is a frequent association (12) (Fig. 3). By contrast, opacities of the *q* and *r* types are characterized by sharply demarcated round nodules or irregular contracted nodules. The nodules may be centrilobular or subpleural in location and tend to predominate in the posterior upper lobes. Subpleural micronodules may become confluent to form a "pseudo-plaque" (13). Approximately 20% of coal workers have irregular opacities suggestive of lung fibrosis, associated with functional impairment (14,15).

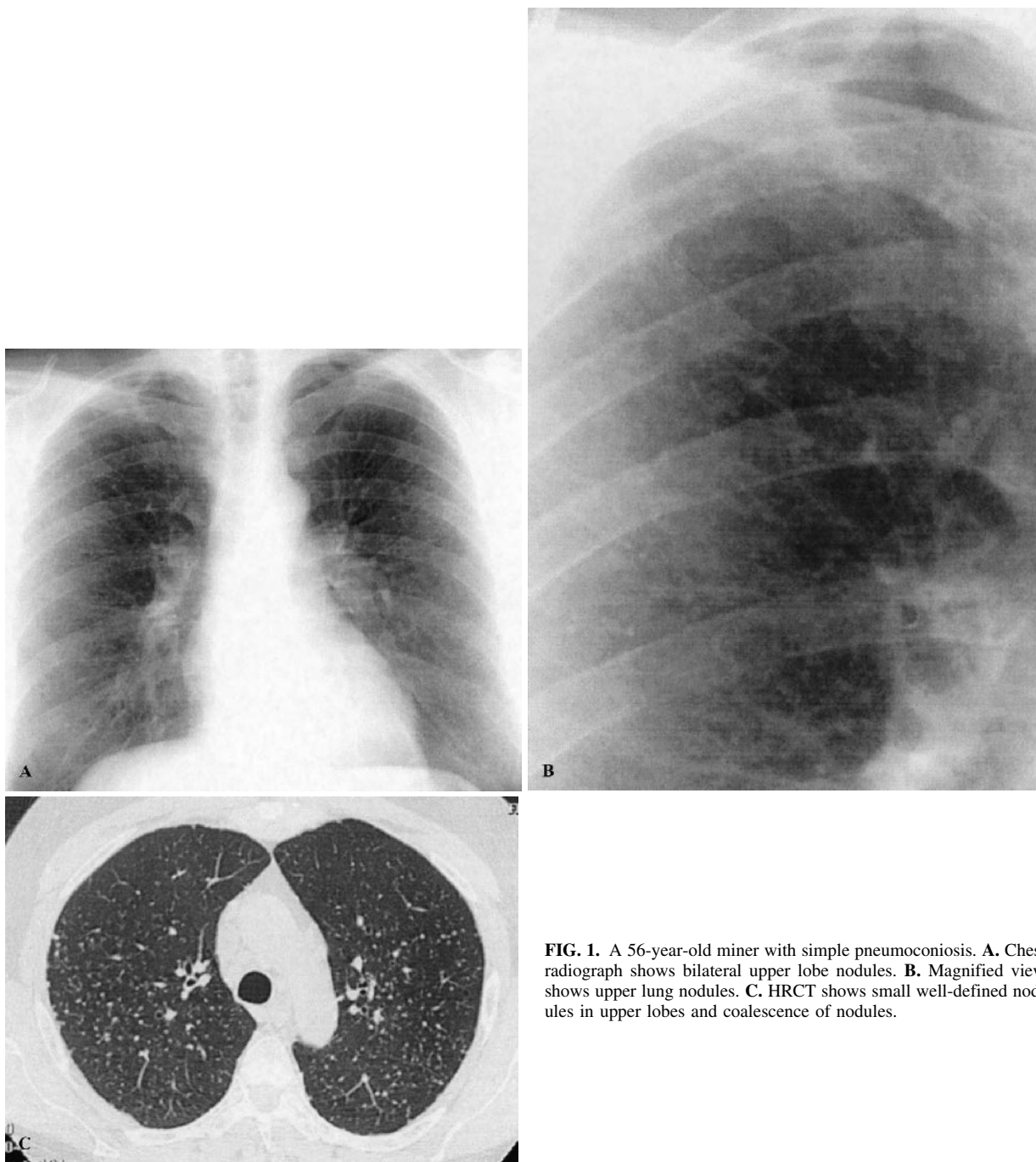


FIG. 1. A 56-year-old miner with simple pneumoconiosis. **A.** Chest radiograph shows bilateral upper lobe nodules. **B.** Magnified view shows upper lung nodules. **C.** HRCT shows small well-defined nodules in upper lobes and coalescence of nodules.

In up to 10% to 20% of silica workers, CT scanning and biopsy have shown changes identical to those of idiopathic pulmonary fibrosis (16–20) (Fig. 4). This apparent association between silica exposure and diffuse lung fibrosis is increasingly recognized (16–19). Patients with diffuse lung fibrosis related to silicosis appear to be at substantially increased risk for development of lung cancer (20).

In silicosis, pulmonary function correlates poorly with

the profusion of nodules on CT, but the CT-determined extent of emphysema correlates well with FEV1 and diffusing capacity (8). Several articles have shown that emphysema develops in a substantial proportion of lifelong nonsmokers exposed to silica. In a CT study of 207 miners with normal or near-normal chest radiographs, emphysema was seen in eight of 11 nonsmokers with pneumoconiosis but in only one of 20 nonsmokers without

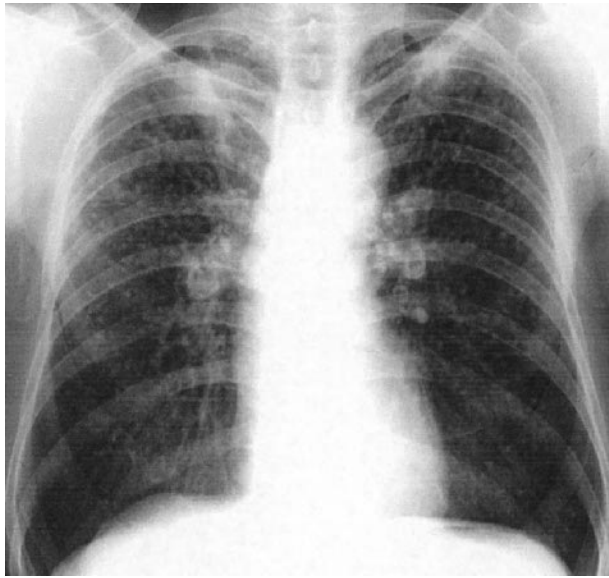


FIG. 2. A 57-year-old miner with eggshell calcifications of lymph nodes. Chest radiograph shows multiple eggshell calcifications of hila and aortopulmonary window lymph nodes. There are bilateral apical masses with upper lobe volume loss compatible with PMF.

pneumoconiosis (21). The presence of pneumoconiosis on CT was a predictor of emphysema extent, and exposure to silica was a significant predictive factor for emphysema even in patients without CT evidence for pneumoconiosis. A study of 70 gold miners by Cowie et al. (22) reached similar conclusions. However, in an autopsy study of lifelong nonsmoking miners, Hnizdo et al. (23) found that the extent of impairment of pulmonary function (FEV1 and FVC) in these nonsmokers was not related to the extent of emphysema present at autopsy but was related to the degree of silicosis. Measures of gas exchange were not included in this study. Computed tomography may be useful in evaluation of individual patients with silicosis, particularly for identifying emphysema or conglomerate masses in those who have substantial pulmonary physiologic impairment without radiographic evidence of complicated silicosis.

In CWP, CT is more sensitive than the chest radiograph for detection of pulmonary nodules, and HRCT is more sensitive than conventional CT for detection of nodules smaller than 3 mm in diameter (12). Importantly, in subjects in whom small, round opacities were identified on the chest radiograph, HRCT was normal in 20% and was minimally abnormal in 42%. Similarly, Gevenois et al. (24) demonstrated that opacities thought to represent pneumoconiosis on the chest radiograph can often be ascribed by CT to bronchiectasis or emphysema. Thus, the chest radiograph may underestimate and overestimate the extent of pneumoconiosis. Distinction of small nodules from vessels is easier on conventional or

spiral CT than on HRCT (25). However, HRCT allows better assessment of fine parenchymal detail and of emphysema. Furthermore, HRCT may allow detection of nodules in patients who have normal radiographic and conventional CT findings (26) and is particularly helpful in the assessment of patients who have nodules smaller than 1.5 mm in diameter (12). With multidetector scanners, use of helical thin-section images allows reconstruction of minimum intensity projection slabs that may facilitate discrimination of nodules from vessels while maintaining the greater sensitivity of thin CT sections. In a study by Begin et al. (27) of workers with silicosis, CT demonstrated unsuspected early conglomeration in one-third of patients who were classified as having simple silicosis on the basis of the chest radiograph. These subjects had corresponding abnormalities of lung function. Conventional CT and HRCT may also allow detection of early confluence of nodules not apparent on the radiograph (8,26). The interobserver agreement for CT scan readings was markedly higher than for radiographic interpretations (26). Therefore, in the assessment of patients who have possible silicosis, it is recommended that conventional or spiral CT scans be obtained and be supplemented by HRCT scans obtained at three to five levels through the upper lung and mid lung zones (26–28). Alternatively, a multidetector scanner may be used to reconstruct thick section images of the lungs with thin sections at desired levels.

Progressive massive fibrosis, sometimes referred to as complicated pneumoconiosis or conglomerate pneumoconiosis, is much more common in silicosis than in CWP. On the chest radiograph, PMF presents with mass-like or sausage-shape opacities, typically seen in the posterior upper lobes, with associated hilar retraction (Fig.

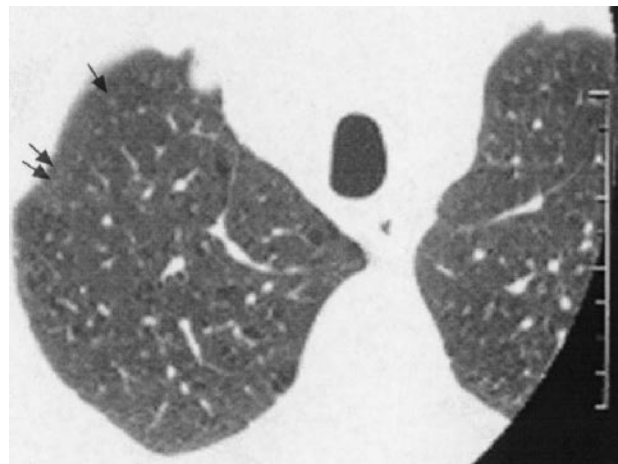


FIG. 3. A 55-year-old man with type *p* pneumoconiosis. HRCT shows small poorly defined nodules (arrows) associated with centrilobular emphysema.

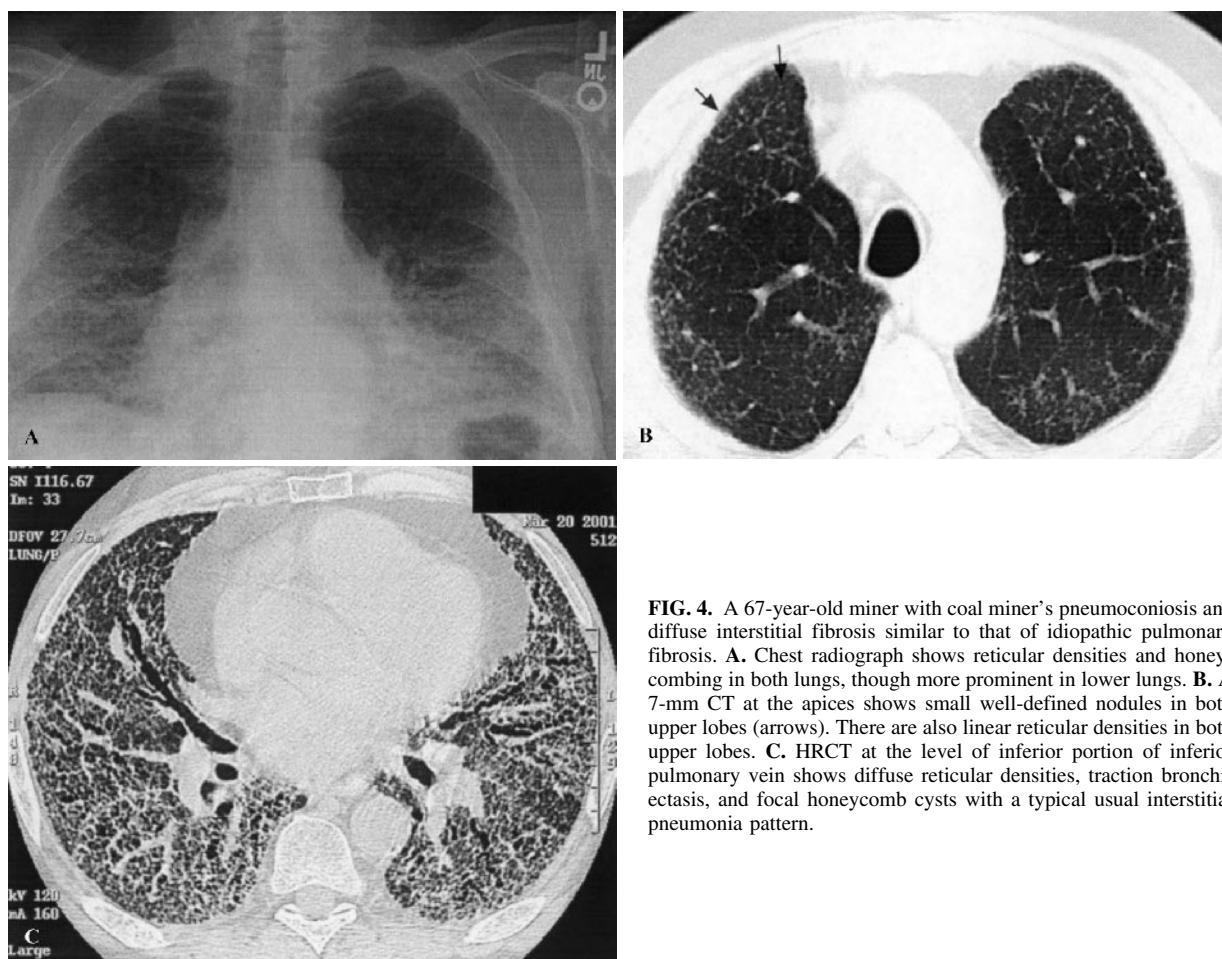


FIG. 4. A 67-year-old miner with coal miner's pneumoconiosis and diffuse interstitial fibrosis similar to that of idiopathic pulmonary fibrosis. **A.** Chest radiograph shows reticular densities and honeycombing in both lungs, though more prominent in lower lungs. **B.** A 7-mm CT at the apices shows small well-defined nodules in both upper lobes (arrows). There are also linear reticular densities in both upper lobes. **C.** HRCT at the level of inferior portion of inferior pulmonary vein shows diffuse reticular densities, traction bronchiectasis, and focal honeycomb cysts with a typical usual interstitial pneumonia pattern.

5). Because the mass-like fibrosis is usually lenticular rather than spherical in shape, it is often less dense than expected on the frontal radiograph. Large opacities in PMF that are clearly separated from the pleura by aerated lung have a characteristic "angel's wing" appearance on the chest radiograph (29). Sequential evaluation of these masses often shows apparent migration toward the hila, leaving a peripheral rim of cicatricial emphysema. Although usually symmetric, masses may be unilateral. Unilateral PMF may be distinguished from lung cancer by the presence of lobar volume loss and peripheral emphysema. On CT, PMF typically appears as a mass of upper and posterior portions of the lung (often bilateral) with irregular borders, frequent calcification, and surrounding cicatricial emphysema (Fig. 5). Thickening of the adjacent extrapleural fat is common. A central area of low density is often seen in masses that are larger than 4 cm in diameter and likely represents necrosis. Cavitation is a less frequent finding. Various types of calcifications can be observed, mostly punctate rather than linear or massive (30). The presence of necrosis or cavitation in

PMF should always raise the suspicion of tuberculous or atypical mycobacterial superinfection.

When mycobacterial infection and silicosis coexist, the diagnosis may be difficult, because silicotic nodules may become engulfed by the tuberculous process and basilar hyperinflation or emphysema may obscure the telltale small, round silicotic opacities. Opacities caused by mycobacterial or fungal infection, in contrast to those of PMF, tend to abut the pleura and incite pleural thickening. The presence of multiple, small, round opacities remote from the tuberculous process facilitates the concurrent diagnosis of pneumoconiosis in the presence of mycobacterial infection (29) (Fig. 6).

Asbestos-Related Diseases

Exposure to asbestos is an important public health hazard in all industrial societies. The problem has been a topic of widespread public interest, in part because of the ubiquity of this material in daily life and also because of the association of pulmonary fibrosis and malignant disease with the inhalation of the fibers (31).

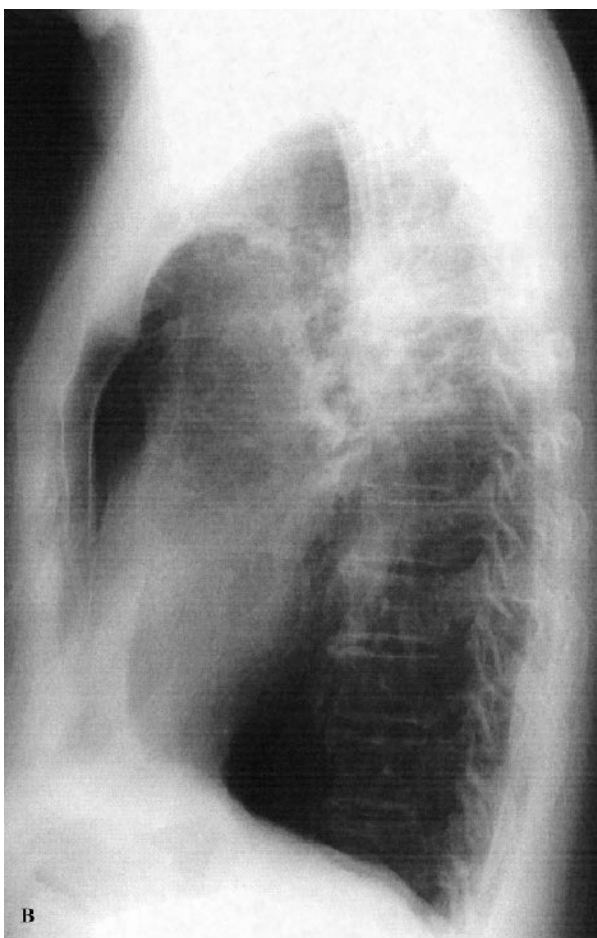
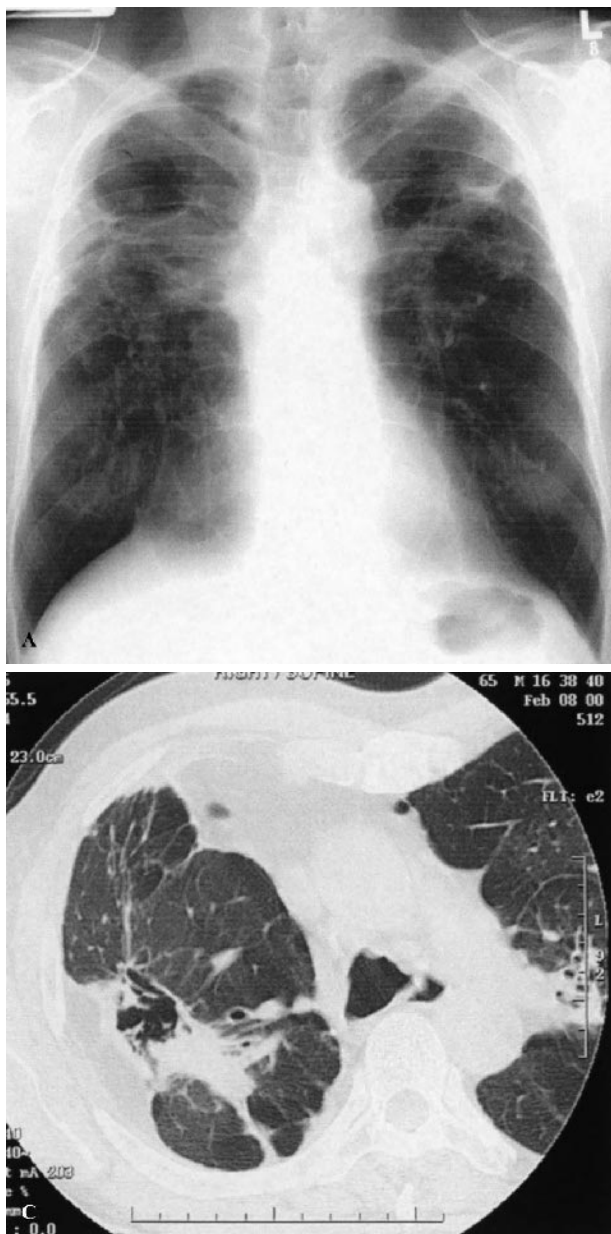


FIG. 5. A 66-year-old miner with PMF. **A,B.** Frontal and lateral chest radiographs show bilateral upper lobe mass-like opacities with peripheral bullae and superior displacement of both hila. Small nodules are present in upper and mid lung zones. The lateral view shows the masses to be in the typical posterior location. **C.** HRCT shows the fibrotic mass in the posterior right upper lobe. There is peripheral emphysema and thickening of the adjacent extrapleural fat.

The role of chest radiology in assessment of asbestos exposure is two-fold: 1) to document the presence or absence of pleural disease as a marker of asbestos exposure; and 2) to ascertain the presence and extent of com-

plications of asbestos exposure, including asbestosis, lung cancer, malignant mesothelioma, pleural abnormalities, and benign asbestos-related lung masses.

The presence and type of radiographic abnormality in

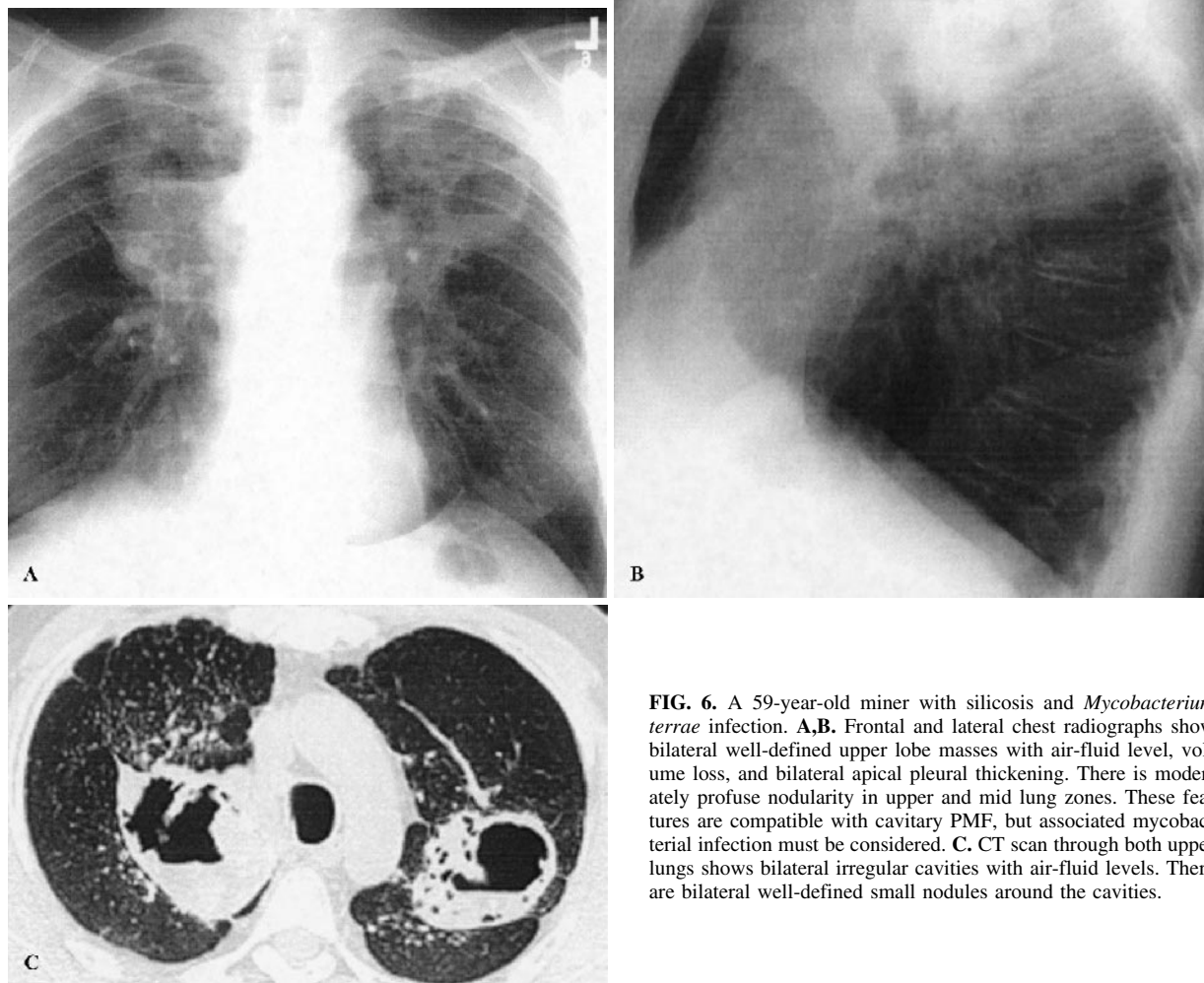


FIG. 6. A 59-year-old miner with silicosis and *Mycobacterium terrae* infection. **A,B.** Frontal and lateral chest radiographs show bilateral well-defined upper lobe masses with air-fluid level, volume loss, and bilateral apical pleural thickening. There is moderately profuse nodularity in upper and mid lung zones. These features are compatible with cavitory PMF, but associated mycobacterial infection must be considered. **C.** CT scan through both upper lungs shows bilateral irregular cavities with air-fluid levels. There are bilateral well-defined small nodules around the cavities.

asbestos-exposed workers depends on the interval since exposure began (latency) and the duration and intensity of the exposure. Table 1 provides an illustration of the latency and relative frequency of the pleural and parenchymal manifestations of asbestos exposure. Clearly, the incidence and prevalence of these abnormalities will vary widely depending on the population being studied, the severity of exposure, and the diagnostic criteria used.

Asbestos-Related Pleural Disease

There are four distinct types of asbestos-related pleural disease. Benign asbestos-related pleural effusion has

the shortest latency (5–20 years) but is the least common. Pleural plaques are the most common manifestation of asbestos exposure. Diffuse pleural thickening is less common. Finally, malignant mesothelioma is one of the most feared, though least common, manifestations of asbestos exposure. Round atelectasis is an effect of asbestos-induced pleural disease.

Benign Asbestos-Related Pleural Effusion

Benign asbestos-related pleural effusion may be identified as an incidental finding on chest radiograph (32,33). Unlike pleural plaques, asbestos pleurisy in-

TABLE 1. *Pleuropulmonary complications of asbestos exposure**

Abnormality	Latency (years)	Approximate frequency in asbestos-exposed workers (%)
Benign pleural effusion	5–20	3
Pleural plaques	15–30	16–80
Calcified pleural plaques	20–40	10–50
Diffuse pleural thickening	10–40	7–13
Asbestosis	20–40	15–30
Lung cancer	>15	20–40 (lifetime risk)
Mesothelioma	15–40	10 (lifetime risk)

* Reproduced with permission from Lynch DA, Newell JD, Lee JS eds. *Imaging of diffuse lung disease*. Ontario: BC Decker; 2000:141–169.

volves the visceral and the parietal pleura and may be associated with symptoms and pulmonary function impairment (34). The effusions are usually exudative and may be bloodstained. The prevalence of effusions is 3.1% (32,35) and appears to increase as the level of exposure increases. At least two-thirds are asymptomatic. The diagnosis of benign asbestos-related pleural effusion is often problematic. To be classified as a benign effusion, it must remain clinically benign for at least 3 years; therefore, the diagnosis must remain suspect for at least this period (32). A number of cases of pleural effusion initially thought to be benign ultimately are identified to be caused by mesothelioma.

Radiologically, these effusions are often small, may be persistent or recurrent, and may be simultaneously or sequentially bilateral (33) (Fig. 7). The radiographic or CT features are not specific, and CT is not usually required for the detection of pleural effusion; however, the higher CT attenuation of free blood within the pleural cavity may suggest the bloody nature of asbestos-related pleural effusion (36). The latency of benign asbestos-related pleural effusion is often shorter than that of other asbestos-related pleural disease, frequently occurring within the first 10 years after initial asbestos exposure. Benign asbestos-related pleural effusions may be associated with rounded atelectasis and with linear fibrotic strands radiating to the surrounding lung (37). However, these findings may occur in relation to any chronic pleural process, including mesothelioma. Benign asbestos-related pleural effusions must be differentiated from other causes of chronic pleural effusion, including infection, trauma, and malignancy. Diffuse pleural thickening, with impairment of pulmonary function, is a common sequela of benign asbestos-related pleural effusion (38), but the role of decortication in preventing this complication is unclear.

Pleural Plaques

Pleural plaques are the most common manifestation of asbestos exposure. They serve as a marker of exposure

and may be seen with brief or slight exposure. Although the overall incidence of plaques increases with dose, a linear correlation does not exist between plaque severity and total dust exposure (39). Pleural plaques are focal

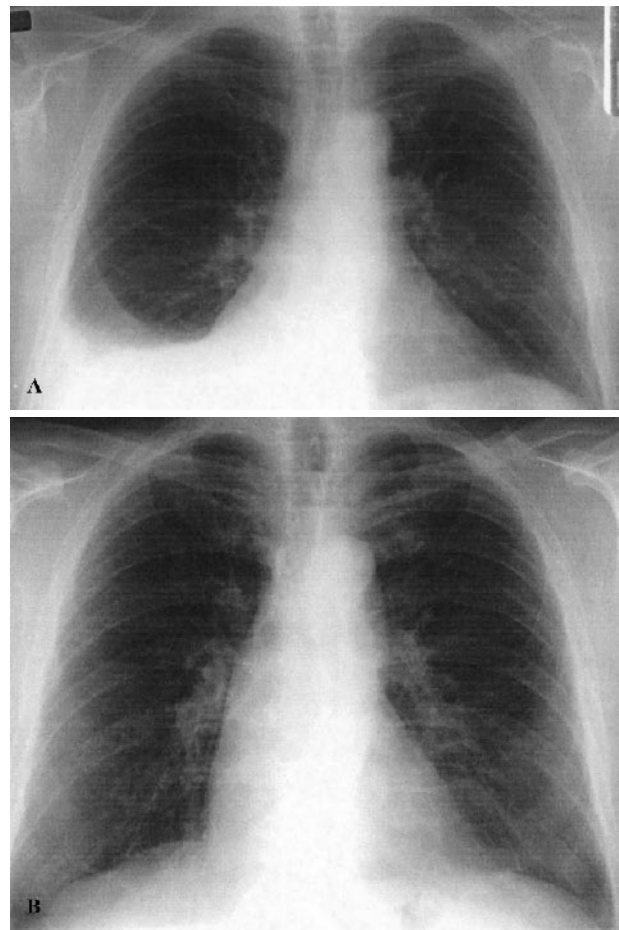


FIG. 7. A 65-year-old asbestos worker with benign asbestos-related pleural effusion. **A.** Chest radiograph shows moderate, asymptomatic, right effusion. **B.** Follow-up chest radiograph 5 years later shows clearing of effusion but residual blunting of the right costophrenic sulcus indicating pleural thickening. Reproduced with permission from Lynch DA, Newell JD, Lee JS, eds. *Imaging of diffuse lung disease*. Ontario: BC Decker, 2000:141–169.

smooth areas of pleural thickening that predominantly involve the parietal pleura. Plaques usually do not form in the visceral pleura (Fig. 8). However, calcified and noncalcified plaques may occur in the interlobar fissures (40,41). Calcification is seen in approximately 15% of patients with plaques.

Noncalcified pleural plaques are difficult to identify on the chest radiograph except when the x-ray beam is tangential to the plaque. The plaque appears in profile as a sharply marginated dense band of soft tissue ranging from 1 to 10 mm in thickness, paralleling the inner margin of the lateral thoracic wall (Fig. 9). Plaques are usually bilateral, often symmetric, and more prominent in the lower half of the thorax between the sixth and ninth ribs (42). For unexplained reasons, pleural plaques are more prevalent on the left than on the right (43). Noncalcified diaphragmatic plaques are sometimes seen as well-defined focal protrusions from a diaphragmatic

pleural surface and must be distinguished from the less well-defined muscular thickening of the diaphragm.

It is important to differentiate between noncalcified plaques and extrapleural fat (44). Typically, extrapleural fat is seen in profile on the chest radiograph as smooth or wavy thickening of the extrapleural soft tissues (Fig. 10). It may be distinguished from noncalcified pleural plaque by its slightly greater radiolucency and by the fact that it usually extends as a continuous interface into the lung apices. Neither fat nor plaque usually involves the costophrenic sulci, a feature that distinguishes them from diffuse pleural thickening that typically causes blunting of the costophrenic sulci. Use of oblique radiographs has previously been suggested as a method for improving the detection of pleural plaques (45), but this may result in a large number of false-positive diagnoses of pleural fibrosis, because of the presence of extrapleural fat (46). In individual cases, CT may be needed to distinguish be-

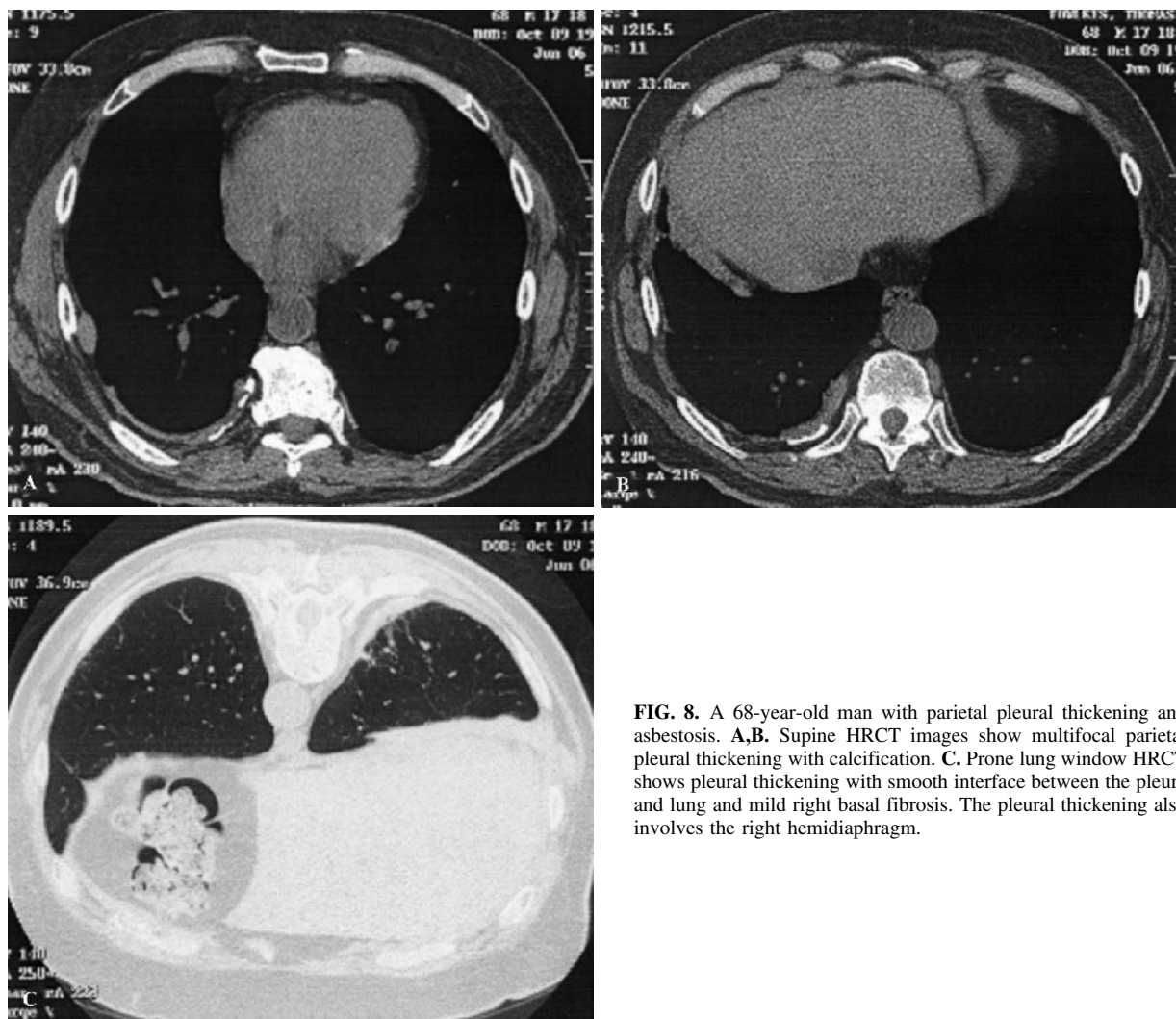


FIG. 8. A 68-year-old man with parietal pleural thickening and asbestosis. **A,B.** Supine HRCT images show multifocal parietal pleural thickening with calcification. **C.** Prone lung window HRCT shows pleural thickening with smooth interface between the pleura and lung and mild right basal fibrosis. The pleural thickening also involves the right hemidiaphragm.

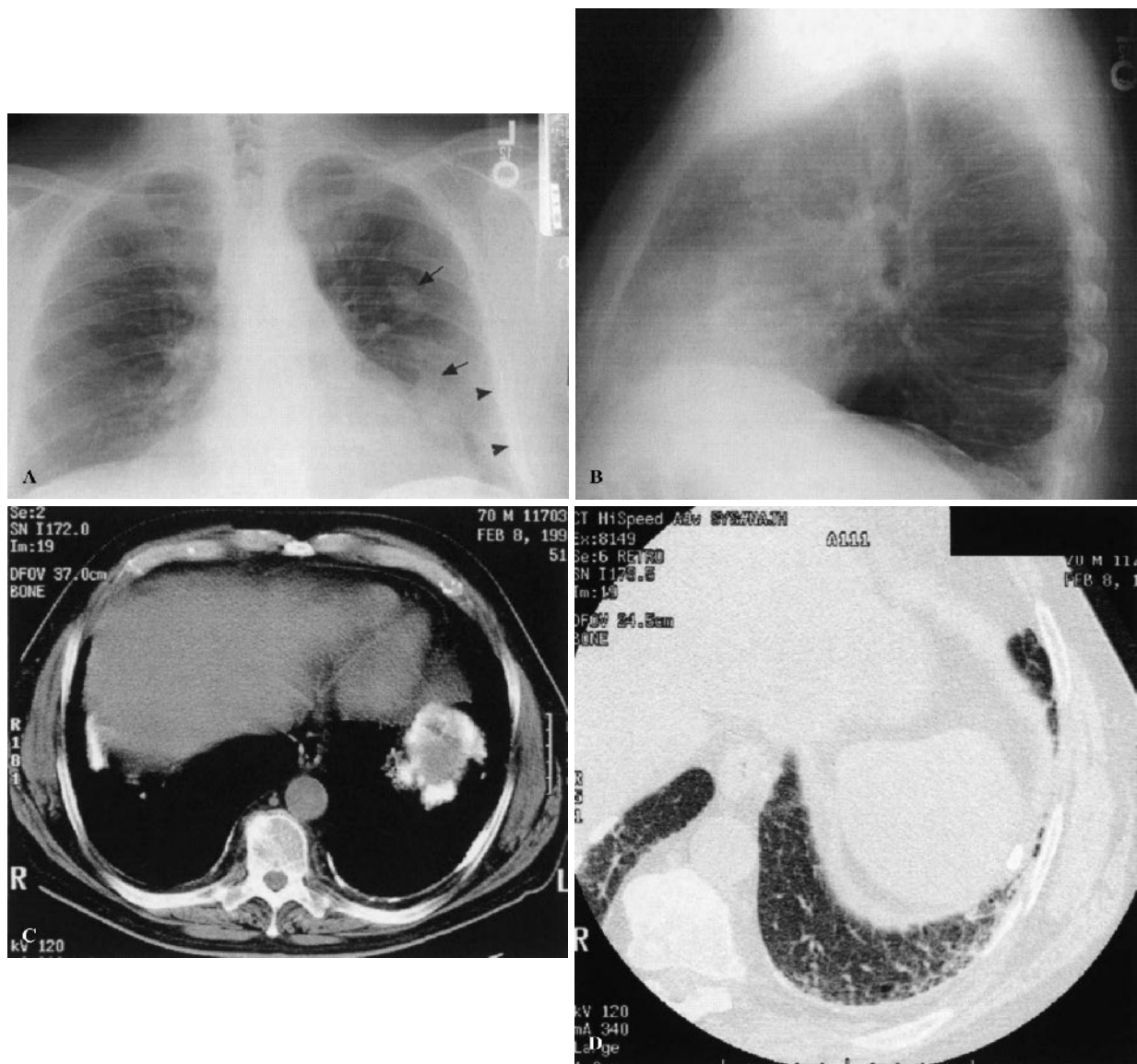


FIG. 9. A 70-year-old man with pleural plaques and asbestosis. **A,B.** Frontal and lateral chest radiographs show multiple en face pleural plaques (arrows) and plaques in profile along the left lateral chest wall (arrowheads). Linear pleural calcification is evident along each hemidiaphragm. **C.** Conventional CT shows diffuse pleural thickening and calcification. Nodular pleural calcification is evident along each hemidiaphragm. **D.** HRCT shows basal reticular densities consistent with asbestosis.

tween extrapleural fat and noncalcified plaques, but this distinction is often clinically unimportant, because asbestos exposure can usually be confirmed from the patient's history.

Calcified pleural plaques may be seen either in profile, as linear areas of calcific density along the chest wall, or en face, as irregularly outlined areas of calcification, sometimes having a "holly leaf" appearance.

Computed tomography scanning is more sensitive than the chest radiograph for detection of pleural plaques (47,48), particularly noncalcified pleural plaques.

Plaques are identified on CT by the presence of smooth soft tissue thickening along the chest wall (Fig. 11). Plaques can be distinguished from intercostal muscles and intercostal vessels by HRCT. The sensitivity of CT for detection of pleural plaques depends on the sampling interval. An article by Gamsu et al. (49) showed that asbestosis might be present even when plaques are not seen on HRCT (performed at 4-cm intervals). To optimize detection of plaques on CT, one must image the thorax contiguously by conventional CT in addition to using selective high-resolution imaging (50).

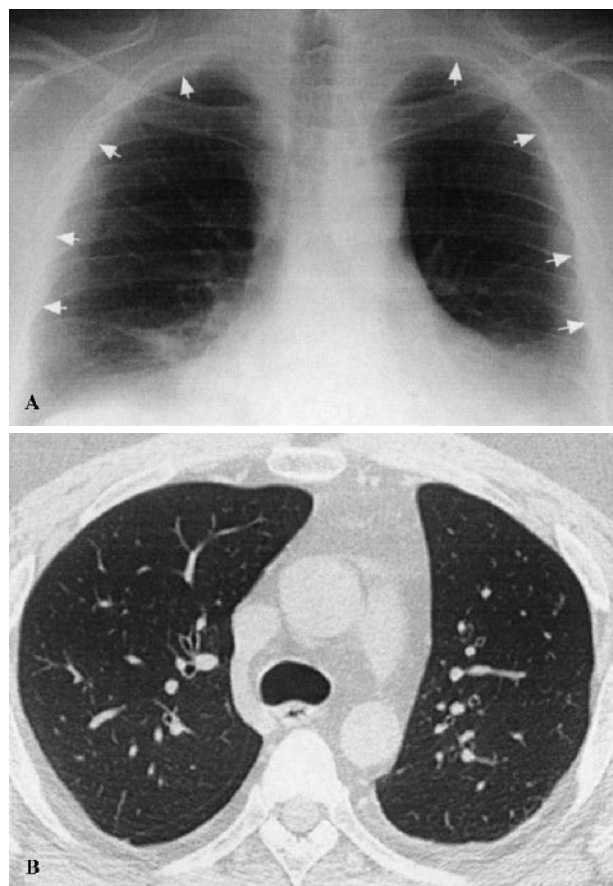


FIG. 10. A 36-year-old man with extrapleural fat. **A.** Chest radiograph shows smooth, wavy thickening of the extrapleural soft tissue (arrows). **B.** HRCT shows diffuse smooth and wavy fat deposition along the posterolateral chest wall bilaterally.

Diffuse Pleural Thickening

Diffuse pleural thickening is less frequently seen than pleural plaques after exposure to asbestos (35,42). There are variable definitions for diffuse pleural thickening. In the ILO classification system, it is defined as pleural thickening extending out of the costophrenic angle and associated with blunting of the sulcus. McLoud et al. (51) have defined it as noninterrupted pleural density extending over at least one-fourth of the chest wall, with or without costophrenic angle obliteration. Because patients with diffuse pleural thickening with a blunted costophrenic angle have more significant functional impairment, the ILO definition is probably the most useful (51). Diffuse pleural thickening is usually presumed to be related to a previous asbestos-related effusion and is often associated with rounded atelectasis.

On chest radiograph, diffuse pleural thickening is characterized by a uniform homogenous density, smooth contours without nodularity, and, frequently, by obliteration of the costophrenic angle (35,42) (Fig. 12).

On CT, diffuse pleural thickening is diagnosed when the pleural thickening extends more than 8 cm cranio-caudally and is 5 cm wide and 3 mm thick (52) (Fig. 12). Asbestos-related diffuse pleural thickening must be distinguished from the visceral pleural and subpleural fibrosis that occurs in patients with many forms of lung fibrosis (including asbestosis). Pure parietal pleural thickening is usually sharply defined on CT, whereas visceral pleural fibrosis is associated with fine fibrous strands extending into the underlying lung, giving a “blurred” or “fluffy” demarcation to the pleural process (36,53). Vis-

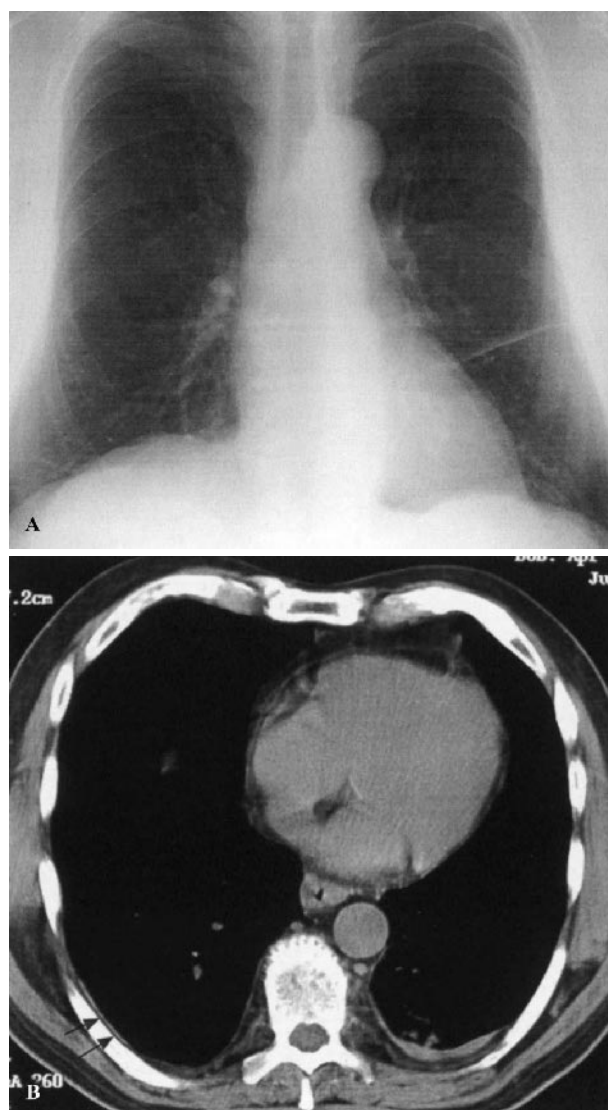


FIG. 11. A 67-year-old man with noncalcified pleural plaque. **A.** Chest radiograph shows no definite evidence of pleural plaque but focal scarring in left lower lobe. **B.** Conventional CT shows localized smooth soft tissue thickening along the posterior left chest wall. Minimal pleural thickening is seen overlying a rib along the right posterolateral chest wall (arrows).

eral pleural fibrosis is usually, but not always, associated with other evidence of lung fibrosis. Visceral pleural/subpleural fibrosis can sometimes be identified on the chest radiograph as thickening of the interlobar fissures (scored as “pi” in the ILO classification system) (40).

Several authors have shown that diffuse pleural thickening on the chest radiograph is associated with restrictive physiology. Most recently, Kee et al. (54) showed that the presence of diffuse pleural thickening on CT is associated with significant decreases in FVC and DLco. Although previous studies have suggested that pleural plaques are not associated with impaired lung function, there are several recent studies that show that pleural plaque may be associated with significant restriction. In particular, an elegant study by Schwartz et al. (55) that used CT to quantify the three-dimensional extent of pleural plaque showed that the extent of pleural plaque was associated with decrease in total lung capacity, independent of any lung fibrosis.

Asbestosis

The most significant change that occurs in the lung parenchyma secondary to asbestos exposure is diffuse interstitial fibrosis or asbestosis. Several other benign radiographic changes may be observed in the lungs of individuals exposed to asbestos, including round atelectasis, benign fibrotic masses, and parenchymal bands (56). The term asbestosis should be reserved for diffuse lung fibrosis occurring in asbestos-exposed workers. Most workers in whom pulmonary fibrosis develops have been exposed to high dust concentrations for a prolonged period (35). There is a definite dose–effect relationship for asbestosis (57). Asbestosis has been one of the main health hazards related to asbestos exposure, second only to bronchogenic carcinoma in frequency (58,59). Disease usually occurs approximately 20 years after initial exposure. Symptoms include dyspnea and dry cough. Characteristic functional abnormalities consist of progressive reduction of vital capacity and diffusing capacity (56).

The chest radiograph is abnormal in most, but not all, cases of pathologically demonstrated asbestosis (60). The typical radiographic findings in asbestosis are small irregular or reticular opacities, predominating at the lung bases (Fig. 13). Honeycombing is evident in more advanced disease. Pleural plaques are usually present in patients with asbestosis but are absent in approximately 10% of cases (59). A limitation of chest radiographic assessment of asbestosis is the questionable physiologic and pathologic significance of the small irregular opaci-

ties that are the chest radiographic hallmark of early asbestosis (61–64). In at least some cases, these small irregular opacities appear to be related to a combination of cigarette smoke and asbestos exposure.

High-resolution computed tomography is more sensitive than the chest radiograph for diagnosis of the early changes of asbestosis (65–67). Also, HRCT is useful in diagnosing other diseases such as emphysema, which may significantly impair lung function in asbestos-exposed subjects (67). Early asbestosis is manifested on HRCT by peripheral reticular opacities, intralobular



FIG. 12. A 68-year-old asbestos worker with diffuse pleural thickening and asbestosis. **A.** Chest radiograph shows partially calcified pleural thickening extending along most of the left lateral chest wall, associated with decreased volume of the left hemithorax. A calcified plaque is evident in the right mid lung, with a noncalcified en face plaque immediately above it (arrow). **B.** Prone HRCT confirms extensive left basal fibrosis and pleural calcification. Reproduced with permission from Lynch DA, Newell JD, Lee JS, eds. *Imaging of diffuse lung disease*. Ontario: BC. Decker, 2000:141–169.

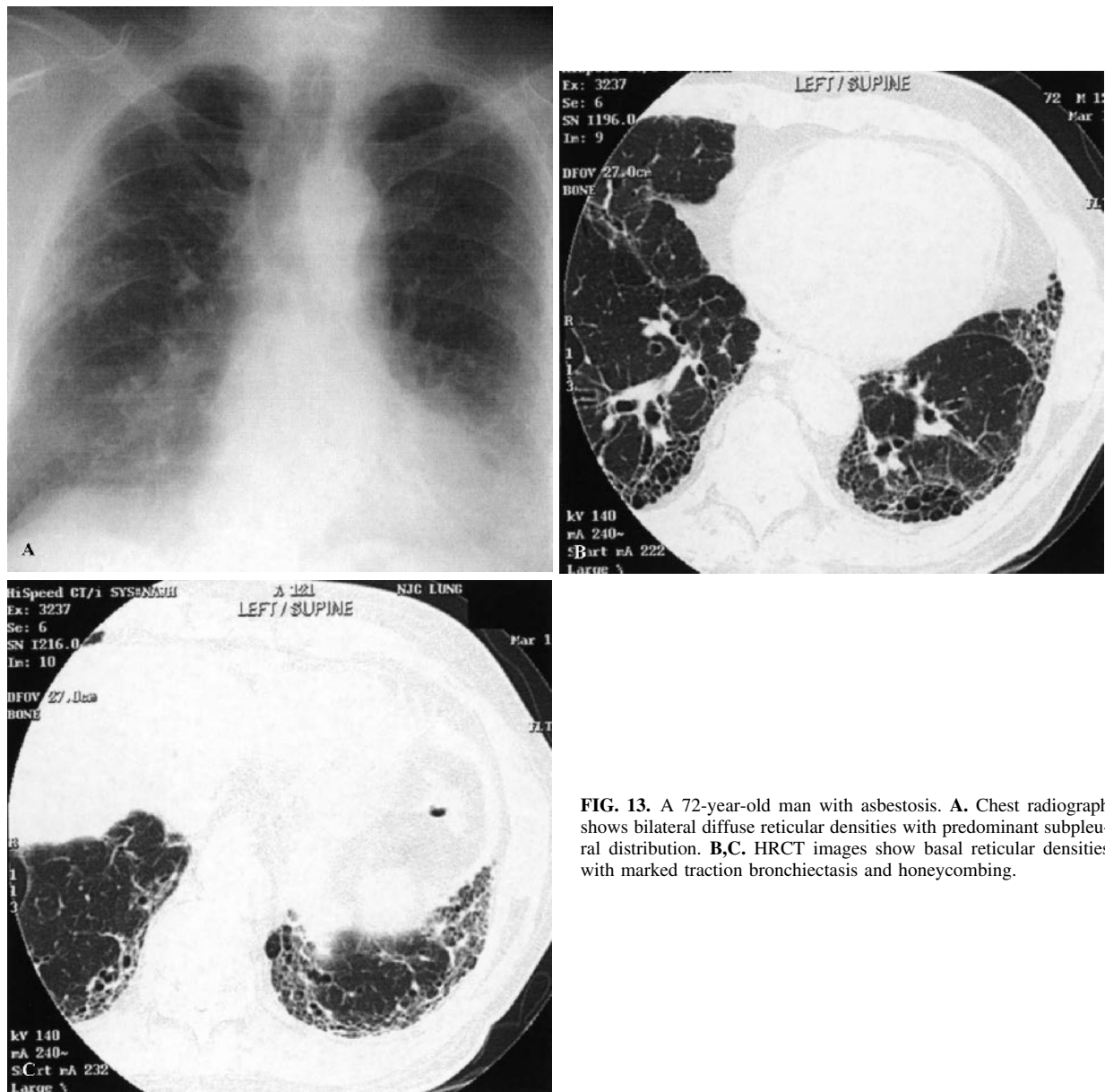


FIG. 13. A 72-year-old man with asbestosis. **A.** Chest radiograph shows bilateral diffuse reticular densities with predominant subpleural distribution. **B,C.** HRCT images show basal reticular densities with marked traction bronchiectasis and honeycombing.

lines, prominent centrilobular core structures, and interlobular septal thickening (Fig. 13). Because of the posterior and basal predominance of the lesions of early asbestosis, examination of the lung bases in the prone position is critical for confirming the fixed nature of septal thickening and curvilinear subpleural lines. More advanced asbestosis is characterized by parenchymal bands of fibrosis, honeycombing, and traction bronchiectasis. Clearly, none of these features is specific for asbestosis, and similar changes may be seen in other lung diseases such as idiopathic pulmonary fibrosis (IPF) (68). When the CT scans of patients with asbestosis are

compared with those of patients with IPF, patients with asbestosis have a higher prevalence of parenchymal bands and a lower prevalence of ground-glass opacities (69).

A study by Aberle et al. (65) evaluated HRCT in 100 asbestos-exposed subjects. They assigned scores for the probability of asbestosis, based on the signs mentioned. This HRCT probability score correlated with forced vital capacity and weakly with lung diffusing capacity. Forty-five of the subjects satisfied clinical criteria for asbestosis; 43 of these had an intermediate- or high-probability HRCT, including eight of 10 subjects with a normal chest radiograph. Interestingly, 30 of the 55 subjects who

did not meet the clinical criteria for asbestosis had an intermediate- or high-probability HRCT. This suggests that the disease detected by HRCT may sometimes be too localized to cause a radiographic abnormality or to affect resting pulmonary function.

A study by Friedman et al. (70) found that HRCT was valuable for eliminating false-positive diagnoses of pleural plaques caused by extrapleural fat and false-positive diagnoses of asbestosis caused by extensive overlying plaques or by emphysema. In contrast to Aberle's study, radiographically occult asbestosis was demonstrated by HRCT in only two of 60 patients in this study. The discrepancies between these studies probably relate to the differences in the severity of asbestosis. Twenty-three percent of those studied by Aberle et al. and 38% of those in Friedman's study had chest radiographic evidence of asbestosis (ILO profusion greater than 1/0).

Do the HRCT features described in early asbestosis represent pathologically and physiologically significant disease? Staples et al. (67) studied HRCT in asbestos-exposed subjects with normal lung parenchyma on chest radiographs. Vital capacity and diffusing capacity (percent predicted) were significantly lower in those who had abnormal HRCT scans. Similarly, in a study by Oksa et al. (71), a HRCT score for parenchymal abnormalities correlated significantly with diffusing capacity and total lung capacity in patients who had normal lung parenchyma on chest radiographs. Neri et al. (72) showed that the presence of parenchymal abnormality on CT was associated with a significantly lower FVC in nonsmoking asbestos-exposed subjects. Thus, parenchymal abnormalities seen on CT in asbestos workers are clearly associated with physiologic impairment, even in those with normal chest radiographs.

Akira et al. (73), in a serial study of 23 asbestos-exposed patients with minimal or no abnormalities on chest radiographs, demonstrated that the changes of early asbestosis progressed in two of seven patients who were reexamined between 10 and 19 months after the first CT scan and in six of eight patients who were examined between 20 and 39 months after the first CT examination. This evidence of progression on CT was accompanied by decrease in lung diffusing capacity in three of four patients in whom serial pulmonary function tests were available. Progression of disease by HRCT criteria appeared to be more prominent in cigarette smokers. Using postmortem HRCT scans, these authors also demonstrated that the centrilobular nodules and branching structures corresponded histologically to fibrosis around the bronchioles, which subsequently involved the alveolar ducts. Pleural-based nodular irregularities corre-

sponded histologically to subpleural fibrosis. Hazy patches of increased attenuation tended to correspond to fibrotic thickening of the alveolar walls and interlobular septae.

A study by Gamsu et al. (49) shows that the CT findings of early asbestosis are neither sensitive nor specific. In a series of 30 patients who had pathologic evaluation for asbestosis, five of nine subjects who had no evidence of asbestosis on CT had histologic asbestosis. Of five further subjects who had minor parenchymal opacities, deemed insufficient in extent and severity for the diagnosis of asbestosis, four had asbestosis. Because most patients in this study had the diagnosis made at autopsy or at lobectomy for malignancy, the population is not representative of the general population with asbestosis. Nevertheless, this study suggests that the borderline between normal and disease is blurred. Gamsu's study also affirms that asbestosis can be diagnosed with confidence when parenchymal changes are bilateral or present at multiple levels. Also, scoring of the profusion of abnormality on CT correlated significantly ($r = 0.78$) with the severity of lung fibrosis on histologic evaluation.

Other Pneumoconioses

Akira et al. (74) have described the CT features in patients with uncommon pneumoconioses. Arc welder's lung may be associated with ill-defined centrilobular micronodules and branching linear structures and is less commonly associated with extensive ground-glass opacities (75) (Fig. 14). Graphite worker's lung is associated with well-defined or ill-defined micronodules, sometimes with septal thickening and larger areas of parenchymal opacity. In aluminum pneumoconiosis, reticular

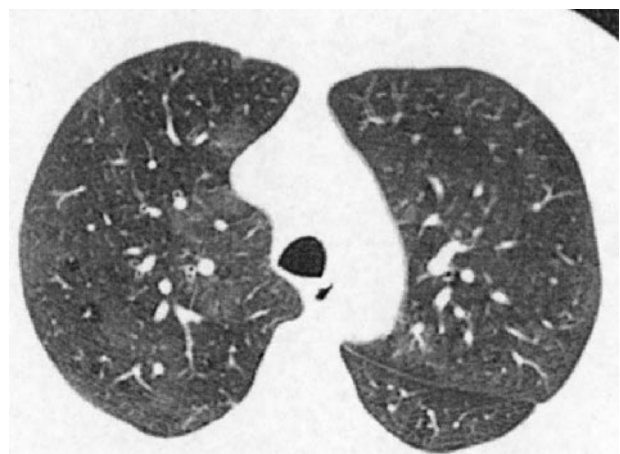


FIG. 14. A 52-year-old man with arc welder's lung. HRCT shows ground-glass attenuation with a few ill-defined nodules.

and small nodular opacities and fibrosis predominate. In hard metal disease, an alloy of tungsten carbide and cobalt and, occasionally, other metals such as titanium and tantalum, one typically sees ground-glass opacification and consolidation, corresponding to the histologic finding of giant cell pneumonitis (74). Although the primary risk from exposure to plutonium is the development of cancers of bone and lung (76), the inhalation of plutonium in gases, dusts, or vapors may also cause lung fibrosis. This property of plutonium has been used to create an animal model of lung fibrosis. The clinical and imaging features of plutonium-related lung fibrosis in humans have not been described. We have seen one patient in whom the imaging appearances were similar to those of idiopathic pulmonary fibrosis (Fig. 15).

BERYLLIOSIS

Beryllium disease is a multisystem disorder caused by exposure to fumes, dusts, or mists of beryllium or its salts. Involvement of lung is the major manifestation of berylliosis. Chronic beryllium disease occurs in a few patients with industrial exposure to beryllium; a type IV hypersensitivity reaction to inhaled beryllium compounds may develop (77).

The radiographic and CT appearances of berylliosis are similar to those of sarcoidosis, though mediastinal and hilar lymphadenopathy is less common. On the chest radiograph, the most common findings were diffuse, small, round areas of opacity, mainly of size *p* or *q*, distributed throughout all the lung fields (78). A mixture



FIG. 15. A 73-year-old man with plutonium lung. A-C. HRCT images show ground-glass attenuation with honeycombing. The honeycombing is more marked in the upper lungs. There is associated emphysema.

of round and irregular areas of opacity was often seen (77,79) (Fig. 16). In advanced disease, coarse linear fibrosis may occur, resulting in progressive loss of volume of involved lung and hilar distortion (80).

On HRCT scans, the appearance of beryllium disease not only includes parenchymal nodules, septal lines, and patches of ground-glass attenuation but also involves the airways, pleura, hilum, and mediastinum (81) (Fig. 16). The nodules are often clustered together around the bronchi or in the subpleural region (81). Calcification in pulmonary nodules has been described (79). Subpleural clusters of nodules may form pseudo-plaques. Ground-glass opacity, bronchial wall thickening, and thickening of interlobular septae are common CT features (80,81). Reticular opacity and architectural distortion may occur, but honeycombing is relatively uncommon. In advanced disease, subpleural cysts may be found. As with other diffuse lung diseases, a normal CT may be seen in patients with biopsy-proven disease. Hilar or mediastinal lymphadenopathy has been described in up to 45% of patients at presentation. Intense calcification of lymphadenopathy has been reported in up to 13% of patients. Pleural thickening is also a recognized feature of chronic berylliosis (77). However, the absence of any abnormality on HRCT scans does not exclude the possibility of beryllium disease (81). In a recent study, the HRCT findings of chronic beryllium disease correlated significantly

(though weakly) with evidence of lung restriction and impaired gas exchange (82).

CHEMICAL PNEUMONITIS AND BRONCHIOLITIS

The inhalation of noxious chemical substances is a comparatively uncommon but significant cause of occupational lung disease. Workers in a variety of occupations are exposed to toxic agents in the form of fume and vapors, as well as aerosols. Occupational history, physical examination, and radiologic imaging form the cornerstones in the diagnosis of chemical pneumonitis (83).

The mechanisms of pulmonary toxicity resulting from different agents vary considerably. Some substances, particularly those that are highly soluble, such as sulfur dioxide, ammonia, and chlorine, are so irritating to the nasal mucosa that individuals may stop breathing on exposure and try to run away. By contrast, less soluble gases, such as phosgene, nitrogen dioxide, ozone, and highly concentrated oxygen, may be inhaled deeply into the lungs before the irritating effect is perceived. Other gases, particularly when inhaled in low concentration, may produce bronchitis or bronchiolitis without the chemical exposure being recognized. Despite these variable characteristics, the concentration of the gas and the duration of the exposure are the chief factors that deter-



FIG. 16. A 46-year-old man with berylliosis. **A.** Chest radiograph shows bilateral small nodules, more prominent in left infrahilar area, with ill-defined opacity. **B.** HRCT shows small well-defined nodules with ground-glass attenuation in left lung. The nodules tend to cluster around the bronchovascular bundles.

mine the form and severity of pulmonary damage and the clinical presentation (84,85). The major injury that results from inhalation of some toxic substances is alveolocapillary damage with resultant permeability pulmonary edema. In others, the chemical injury appears to affect the airways predominantly, resulting in bronchitis and bronchiolitis, sometimes complicated by atelectasis and bacterial pneumonia (84,85). The delayed form of disease is reflected pathologically by obliterative bronchiolitis. This complication can also occur in individuals who initially experience diffuse pulmonary edema (86).

The initial chest radiograph can be normal for as long as 48 hours; therefore, delayed radiographs and extended clinical monitoring are important after significant exposures. The most common radiographic pattern is pulmonary edema, although various radiographic opacities have been reported (Fig. 17). Acute complications in-

clude secondary pneumonia. Long-term complications include bronchiectasis, bronchiolitis obliterans, and lung destruction (83).

Airways Disease

Two distinct types of airways disease may occur after occupational exposure to noxious fumes, gases, or mists. Toxic fumes may induce the development of reactive airways disease, with airway obstruction. On imaging, these patients may show mosaic lung attenuation with air trapping on expiratory imaging (87) (Fig. 18). Constrictive bronchiolitis is an uncommon consequence of occupational exposure to toxic fumes. This clinical entity is most commonly seen in workers exposed to oxides of nitrogen (nitrogen dioxide and nitrogen tetroxide), resulting in silo filler's disease (88). In the acute phase of silo filler's disease, upper airway symptoms may develop. In

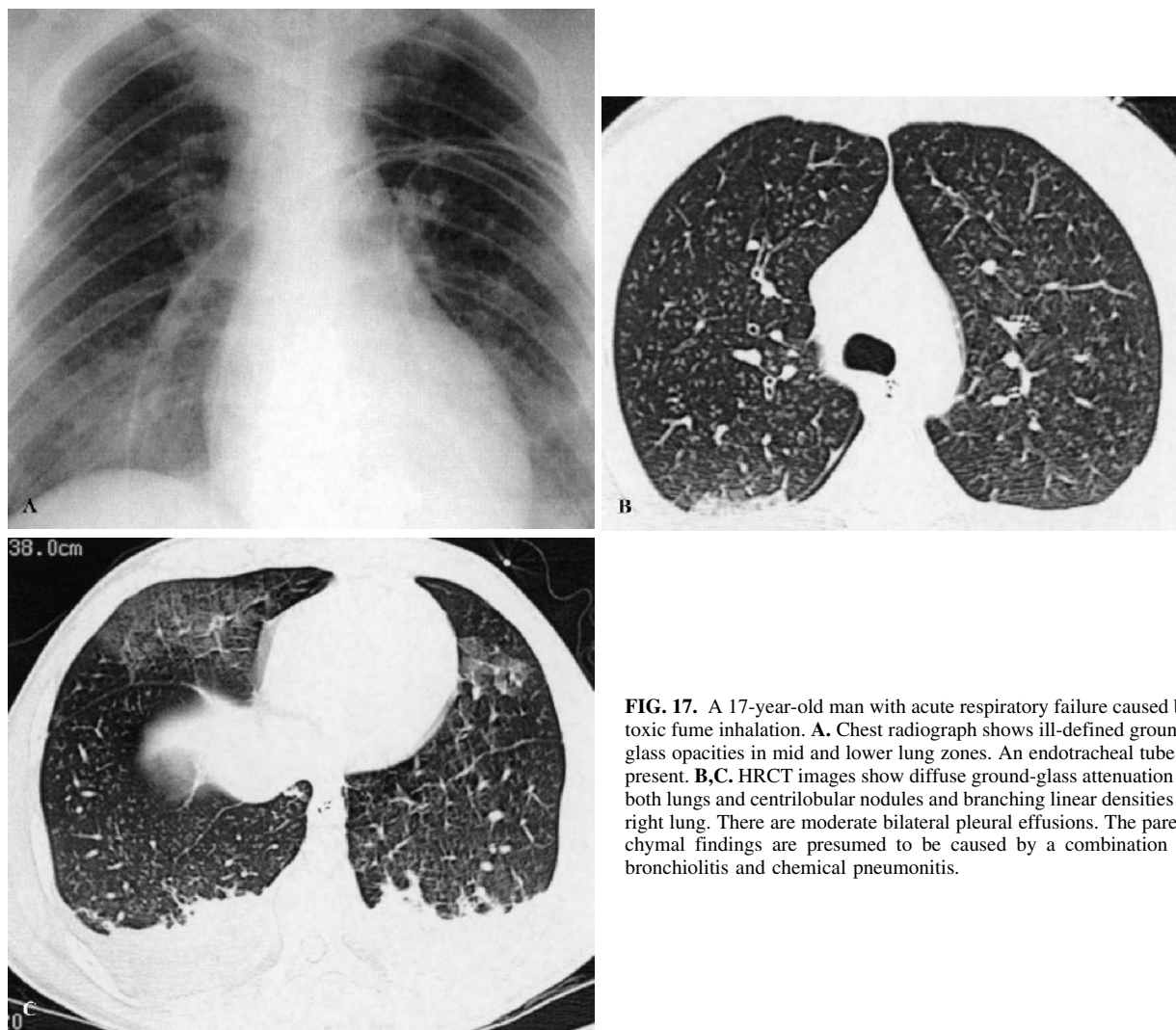


FIG. 17. A 17-year-old man with acute respiratory failure caused by toxic fume inhalation. **A.** Chest radiograph shows ill-defined ground-glass opacities in mid and lower lung zones. An endotracheal tube is present. **B,C.** HRCT images show diffuse ground-glass attenuation in both lungs and centrilobular nodules and branching linear densities in right lung. There are moderate bilateral pleural effusions. The parenchymal findings are presumed to be caused by a combination of bronchiolitis and chemical pneumonitis.

those who survive the acute phase, pulmonary edema (chemical pneumonitis) may develop 3 to 30 hours after exposure. After recovery from this second phase, progressive airway obstruction caused by constrictive bronchiolitis may develop 2 to 6 weeks after exposure. The CT appearances of bronchiolitis obliterans related to toxic fume exposure have not, to our knowledge, been described. Most of the literature dealing with this entity is old, and describes obstructive lung disease developing 3 to 6 weeks after the toxic fume exposure. Because the bronchiolitis is primarily inflammatory, one would expect to see initial changes compatible with a cellular bronchiolitis, progressing later to a pattern consistent with constrictive bronchiolitis, similar to the pattern of constrictive bronchiolitis found in patients with previous viral infection, lung transplantation, or collagen vascular disease (Fig. 19).

FLOCK WORKER'S LUNG

Flock is a fine nylon fiber that is applied to backing to produce the plush material used in luxury upholstery, wallpaper, greeting cards, and many other products. The manufacture of this product may result in a dust of tiny respirable fibers that can reach the alveoli. A respiratory illness called flock worker's lung develops in some flock workers; it is characterized pathologically by a pattern of lymphocytic bronchiolitis and peribronchiolitis with lymphoid hyperplasia (89–91). On HRCT scanning, flock worker's lung is characterized by a combination of ground-glass attenuation and centrilobular nodularity, quite similar to the findings in hypersensitivity pneumonitis or respiratory bronchiolitis (92) (Fig. 20). In symptomatic patients who do not meet current criteria for flock worker's lung, HRCT may identify similar findings.

CLINICAL ROLE OF IMAGING IN OCCUPATIONAL LUNG DISEASE

Screening for Occupational Lung Disease

The chest radiograph is relatively insensitive and nonspecific for detection of occupational lung diseases. Indeed, its lack of sensitivity and specificity leads one to question its continued use in patients with low-level exposures who have a previously low probability of disease. In patients with higher-level exposures, its use may be justifiable, but its lack of specificity, particularly for the diagnosis of asbestosis, suggests that confirmatory imaging or physiologic tests are required when asbestosis is diagnosed on the basis of 1/0 or 1/1 small irregular opacities on the chest radiograph.

Compared with the chest radiograph, chest CT is substantially more sensitive and specific for diagnosis of occupational lung disease. It is also more accurate for detection of complicating conditions such as lung cancer, emphysema, and round atelectasis. However, because pathologic correlation is difficult to obtain in occupational lung disease, we have only fragmentary information about the true sensitivity and specificity of chest CT for diagnosis of pneumoconiosis. It is clear that HRCT may be normal in patients with biopsy-proven occupational lung diseases (49,81,93). Equally clearly, CT can detect significant disease when the chest radiograph is normal (67,81,93). Computed tomography has a major role in screening patients with normal or borderline abnormal chest radiographs for the presence or absence of disease.

Evaluation of Extent of Disease

The profusion of opacities on the chest radiograph, scored on the ILO scale, is commonly used as an objective measure of disease extent. Although this approach may be valid in an epidemiologic study, radiographic profusion in the absence of additional clinical data may be misleading in individual patients. Although CT is more sensitive than the chest radiograph for detection of disease, the lack of standardization of technique and scoring is a major drawback. A standardized CT scoring system analogous to the ILO classification system for chest radiographs must be developed and validated. Objective measures, such as CT lung densitometry, will probably also be useful but will require further validation (94). It is inappropriate to use radiographic profusion or extent of CT abnormality as a surrogate for the degree of functional impairment.

Specific Diagnosis of Occupational Lung Disease

The chest radiograph is relatively nonspecific for diagnosis of many infiltrative lung diseases. Certain findings on HRCT increase the degree of specificity in the correct clinical context. For instance, the finding of profuse, small, poorly defined, centrilobular nodules of the type illustrated in this chapter should be regarded as strongly suggestive of hypersensitivity pneumonitis. The combination of pleural disease and peripheral reticular abnormality or honeycombing strongly supports the diagnosis of asbestosis. The recognition of emphysema on CT can help to explain physiologic impairment that is out of proportion to the degree of radiographic abnormality. The specificity of CT findings is not absolute, and it may be impossible to distinguish hypersensitivity pneumonitis or asbestosis from idiopathic pulmonary fibrosis. In general, radiologic findings should not be regarded as diagnostic of any occupational lung dis-

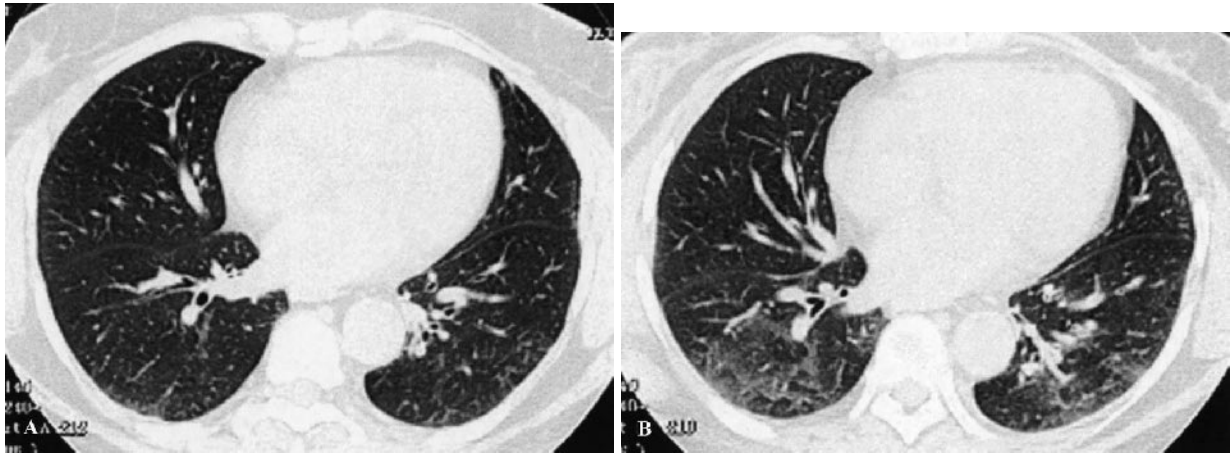


FIG. 18. A. Inspiratory HRCT shows mild mosaic attenuation. B. expiratory HTCT shows patchy airtrapping in both lower lungs.

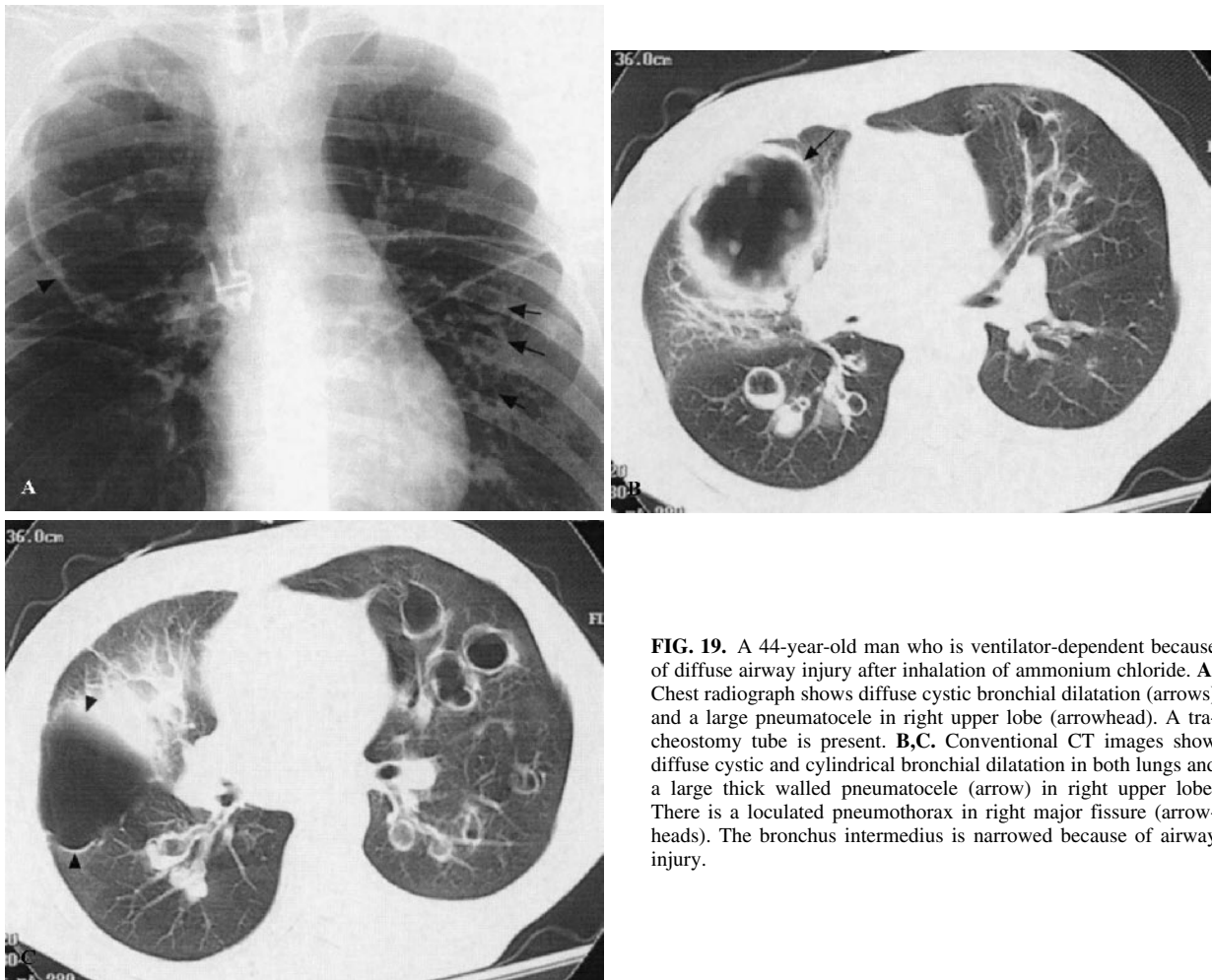


FIG. 19. A 44-year-old man who is ventilator-dependent because of diffuse airway injury after inhalation of ammonium chloride. A. Chest radiograph shows diffuse cystic bronchial dilatation (arrows) and a large pneumatocele in right upper lobe (arrowhead). A tracheostomy tube is present. B,C. Conventional CT images show diffuse cystic and cylindrical bronchial dilatation in both lungs and a large thick walled pneumatocele (arrow) in right upper lobe. There is a loculated pneumothorax in right major fissure (arrowheads). The bronchus intermedius is narrowed because of airway injury.

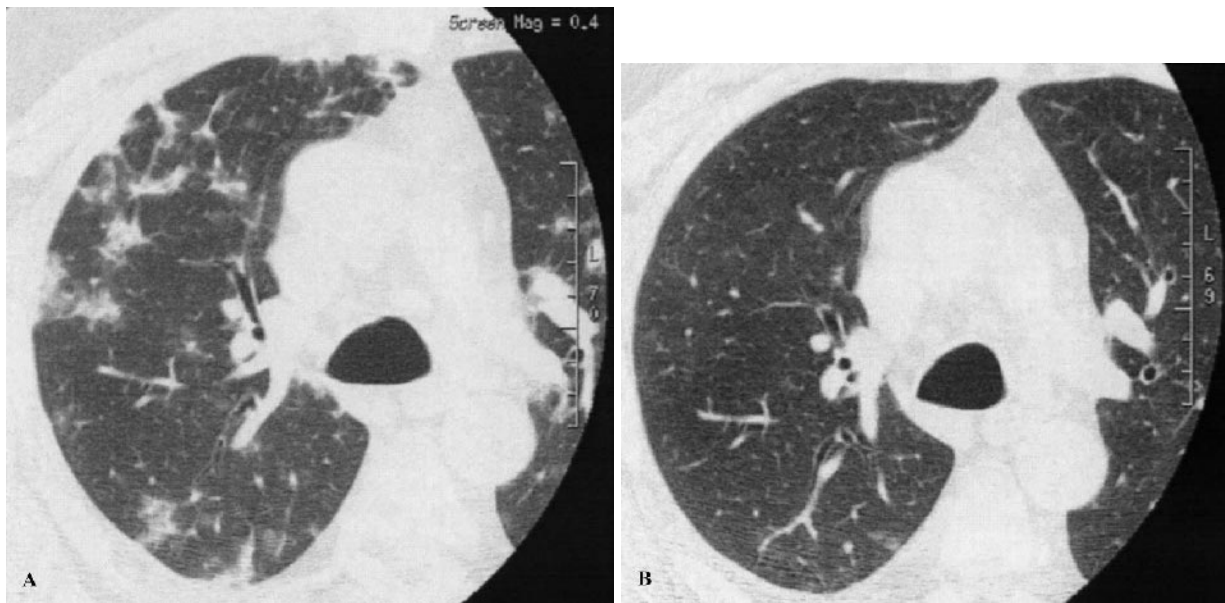


FIG. 20. A 56-year-old man with flock worker's lung. **A.** HRCT shows patchy consolidation with predominant subpleural distribution. Similar to cryptogenic organizing pneumonia. **B.** Follow-up HRCT 3 months later shows much decreased patchy consolidation but residual focal centrilobular ground-glass opacities.

ease without an appropriate supportive history (68,95). In cases in which the history of exposure is unclear or unconvincing, a tissue diagnosis should be vigorously pursued to avoid missing a treatable interstitial lung disease.

Semiquantitative and Quantitative Imaging in Occupational Lung Disease

The ILO classification system is widely used as an epidemiologic tool for semiquantitative assessment of the presence and extent of occupational lung disease on the chest radiograph. However, the chest radiograph is neither sensitive nor specific for detection of infiltrative lung disease, and a validated CT-based quantitative system is urgently required. Semiquantitative scoring systems have been used for scoring the CT extent of disease in patients with silicosis and asbestosis, but these systems have not been validated against the extent of exposure. In a study of asbestos workers by Jarad et al. (96), a CT scoring system was associated with lower interobserver variation than the ILO classification system. In that study, the extent of lung fibrosis and of pleural disease correlated strongly with indices of physiologic impairment. In a study by Schaeffner et al. (97), an index of asbestos exposure was associated with the presence of pleural and parenchymal abnormalities on CT, but the extent of parenchymal disease was not quantified in this study. Oksa et al. (71) evaluated a detailed

CT scoring system in former asbestos sprayers and found significant correlation with DLco and total lung capacity.

Computed tomography has been used to determine the presence of asbestosis in asbestos-exposed workers with borderline abnormal chest radiographs (0/1 or 1/0 by ILO criteria) (98). In these individuals, a normal HRCT scan was associated with normal physiology, whereas an abnormal CT was associated with significantly decreased lung diffusing capacity (DLco). The extent of pulmonary abnormality on CT was significantly (though weakly) correlated with DLco. The extent of pleural disease on CT was associated with decreased forced vital capacity.

Quantitative CT measurement of mean lung density and other CT parameters have also been applied to asbestosis. Wollmer et al. (99) found a significant increase in CT attenuation values in the lungs of 33 asbestos workers, only three of who had evidence of asbestosis on chest radiographs. They found that lung volumes correlated inversely with static lung volumes. Similarly, Reuter et al. (100) showed that asbestos-exposed individuals with normal or near-normal chest radiographs had significantly higher lung density values than age-matched controls, even without visible parenchymal abnormality on CT. This suggests that quantitative CT may detect abnormalities before they are apparent to the eye. In a study of patients with idiopathic pulmonary fibrosis and asbestosis, Hartley et al. (94) showed that measurement of mean lung density and other CT histogram-

derived variables (skewness and kurtosis) correlated with the degree of pulmonary impairment.

REFERENCES

- Banks DE, Parker JE. *Occupational lung disease: An international perspective*. Rochester: Chapman & Hall, 1998.
- Epler GR. Clinical overview of occupational lung disease. *Radiol Clin North Am* 1992;30:1121-1133.
- Fraser RS, Müller NL, Colman N, et al. Inhalation of inorganic dust (Pneumoconiosis). In: Fraser RS, Müller NL, Colman N, et al., eds. *Diagnosis of diseases of the chest*. Philadelphia: WB Saunders, 1999:2386-2484.
- Morgan WRC, Seaton A. *Occupational lung diseases*. Philadelphia: WB Saunders, 1984.
- Bennett JG, Dick JA, Kaplan YS, et al. The relationship between coal rank and the prevalence of pneumoconiosis. *Br J Ind Med* 1979;36:206-210.
- Attfield MD, Althouse RB. Surveillance data on US coal miners' pneumoconiosis, 1970 to 1986. *Am J Public Health* 1992;82:971-977.
- American Thoracic Society. Adverse effects of crystalline silica exposure. *Am J Respir Crit Care Med* 1997;155:761-765.
- Bergin CJ, Müller NL, Vedal S, et al. CT in silicosis: correlation with plain films and pulmonary function tests. *AJR Am J Roentgenol* 1986;146:477-483.
- Guidelines for the use of ILO international classifications of radiographs of pneumoconioses*. Occupational safety and health series. Geneva: International Labor Office, 1990.
- Jacobson G, Felson B, Pendergrass EP, et al. Eggshell calcifications in coal and metal workers. *Semin Roentgenol* 1967;2:276-282.
- Jacobs LG, Gerstl B, Hollander AG, et al. Intraabdominal eggshell calcifications due to silicosis. *Radiology* 1956;67:527-530.
- Akira M, Higashihara T, Yokoyama K, et al. Radiographic type P pneumoconiosis: high-resolution CT. *Radiology* 1989;171:117-123.
- Remy-Jardin M, Beuscart R, Sault MC, et al. Subpleural micronodules in diffuse infiltrative lung diseases: evaluation with thin-section CT scans. *Radiology* 1990;177:133-139.
- Cockcroft A, Berry G, Cotes JE, et al. Shape of small opacities and lung function in coalworkers. *Thorax* 1982;37:765-769.
- Cockcroft A, Lyons JP, Andersson N, et al. Prevalence and relation to underground exposure of radiologic irregular opacities in South Wales coal workers with pneumoconiosis. *Br J Ind Med* 1983;40:169-172.
- Brichet A, Wallaert B, Gosselin B, et al. Idiopathic-like pulmonary fibrosis in coal workers. *Am J Respir Crit Care Med* 1997;155:A331.
- Brichet A, Wallaert B, Gosselin B, et al. Primary diffuse interstitial fibrosis in coal miners: a new entity? Study group on interstitial pathology of the society of thoracic pathology of the north. *Rev Mal Respir* 1997;14(4):277-285.
- McConnochie K, Green FHY, Vallyathan V, et al. Interstitial fibrosis in coal workers: experience in Wales and West Virginia. *Ann Occup Hyg* 1988;32:553-560.
- Green FHY, Vallyathan V. Coal workers' pneumoconiosis and pneumoconiosis due to other carbonaceous dusts. In: Churg A, Green FHY eds. *Pathology of occupational lung disease*. Baltimore: Williams & Wilkins, 1998:129-207.
- Katabami M, Dosaka-Akita H, Honma K, et al. Pneumoconiosis-related lung cancers: preferential occurrence from diffuse interstitial fibrosis-type pneumoconiosis. *Am J Respir Crit Care Med* 2000;162:295-300.
- Begin R, Filion R, Ostiguy G. Emphysema in silica- and asbestos-exposed workers seeking compensation: a CT scan study. *Chest* 1995;108:647-655.
- Cowie RL, Hay M, Thomas RG. Association of silicosis, lung dysfunction, and emphysema in gold miners. *Thorax* 1993;48:746-749.
- Hnizdo E, Sluis CG, Baskind E, et al. Emphysema and airway obstruction in non-smoking South African gold miners with long exposure to silica dust. *Occup Environ Med* 1994;51:557-563.
- Gevenois PA, Pichot E, Dargent F, et al. Low grade coal worker's pneumoconiosis: comparison of CT and chest radiography. *Acta Radiol* 1994;35:351-356.
- Mathieson JR, Mayo JR, Staples CA, et al. Chronic diffuse infiltrative lung disease: comparison of diagnostic accuracy of CT and chest radiography. *Radiology* 1989;171:111-116.
- Begin R, Ostiguy G, Fillion R, et al. Computed tomography in the early detection of silicosis. *Am Rev Respir Dis* 1991;144:697-705.
- Begin R, Bergeron D, Samson L, et al. CT assessment of silicosis in exposed workers. *AJR Am J Roentgenol* 1987;148:509-514.
- Remy-Jardin M, Remy J, Farre I, et al. Computed tomographic evaluation of silicosis and coal worker's pneumoconiosis. *Radiol Clin North Am* 1992;30:1155-1176.
- Stark P, Jacobson F, Shaffer K. Standard imaging in silicosis and coal worker's pneumoconiosis. *Radiol Clin North Am* 1992;30:1147-1154.
- William JL, Moller GA. Solitary mass in the lungs of coal miners. *AJR Am J Roentgenol* 1973;117:765-770.
- Hanson RR, Kasik JE. The pneumoconioses. *Heart Lung* 1977;6:646-652.
- Epler G, McLoud T, Gaensler E. Prevalence and incidence of benign asbestos pleural effusion in a working population. *JAMA* 1982;247:617-622.
- Hillerdal G. Non-malignant asbestos pleural disease. *Thorax* 1981;669-675.
- Wright PH, Hanson A, Kreef L, et al. Respiratory function changes after asbestos pleurisy. *Thorax* 1980;35:31-36.
- McLoud TC. Asbestos-related diseases: the role of imaging techniques. *Postgrad Radiol* 1989;75:3-37.
- Solomon A. Radiological features of asbestos-related visceral pleural changes. *Am J Ind Med* 1991;19:339-355.
- Martensson G, Hagberg S, Pettersson K, et al. Asbestos pleural effusion: a clinical entity. *Thorax* 1987;42:646-651.
- Hillerdal G. Asbestos-related pleural disease. *Semin Respir Med* 1987;9:65-74.
- Wain SL, Roggli VL, Foster WL. Parietal pleural plaques, asbestos bodies, and neoplasia: a clinical, pathologic, and roentgenographic correlation of 25 consecutive cases. *Chest* 1984;86:707-713.
- Rockoff S, Kagan E, Schwartz A, et al. Visceral pleural thickening in asbestos exposure: the occurrence and implications of thickened interlobar fissures. *J Thorac Imaging* 1987;2:58-66.
- Solomon A, Sluis-Cremer GK, Goldstein B. Visceral pleural plaque formation in asbestosis. *Environ Res* 1979;19:258-264.
- Sargent EN, Gordonson J, Jacobson G. Bilateral pleural thickening: a manifestation of asbestos dust exposure. *AJR Am J Roentgenol* 1978;131:579-585.
- Hu H, Beckett L, Kelsey K, et al. The left-sided predominance of asbestos-related pleural disease. *Am Rev Respir Dis* 1993;148:981-984.
- Sargent E, Boswell W, Ralls P, et al. Subpleural fat pads in patients exposed to asbestos: distinction from non-calcified pleural plaques. *Radiology* 1984;152:273-277.
- Baker E, Greene R. Incremental value of oblique chest radiographs in the diagnosis of asbestos-induced pleural disease. *Am J Ind Med* 1982;3:17-22.
- Ameille J, Brochard P, Brechot JM, et al. Pleural thickening: a comparison of oblique chest radiographs and high-resolution computed tomography in subjects exposed to low levels of asbestos pollution. *Int Arch Occup Environ Health* 1993;64:545-548.
- Aberle DR, Gamsu G, Ray CS. High-resolution CT of benign

- asbestos-related diseases: clinical and radiographic correlation. *AJR Am J Roentgenol* 1988;151:883-891.
48. Im J-G, Webb W, Rosen A, et al. Costal pleura: appearances at high-resolution CT. *Radiology* 1989;171:125-131.
 49. Gamsu G, Salmon CJ, Warnock ML, et al. CT quantification of interstitial fibrosis in patients with asbestosis: a comparison of two methods. *AJR Am J Roentgenol* 1995;164:63-68.
 50. Gevenois PA, De VP, Dedeire S, et al. Conventional and high-resolution CT in asymptomatic asbestos-exposed workers. *Acta Radiol* 1994;35:226-229.
 51. McLoud TC, Woods BO, Carrington CB, et al. Diffuse pleural thickening in an asbestos-exposed population: prevalence and causes. *AJR Am J Roentgenol* 1985;144:9-18.
 52. Lynch D, Gamsu G, Aberle D. Conventional and high-resolution CT in the diagnosis of asbestos-related diseases. *Radiographics* 1989;9:523-551.
 53. Hillerdal G, Malmberg P, Hemmingsson A. Asbestos-related lesions of the pleura: parietal plaques compared to diffuse thickening studied with chest roentgenography, computed tomography, lung function, and gas exchange. *Am J Ind Med* 1990;18:627-639.
 54. Kee ST, Gamsu G, Blanc P. Causes of pulmonary impairment in asbestos-exposed individuals with diffuse pleural thickening. *Am J Respir Crit Care Med* 1996;154:789-793.
 55. Schwartz DA, Galvin JR, Yagla SJ, et al. Restrictive lung function and asbestos-induced pleural fibrosis: a quantitative approach. *J Clin Invest* 1993;91:2685-2692.
 56. McLoud T. Conventional radiography in the diagnosis of asbestos-related disease. *Radiol Clin North Am* 1992;30:1177-1189.
 57. Lynch DA, Gamsu G, Ray C, et al. Asbestos-related focal lung masses: manifestations on conventional and high-resolution CT scans. *Radiology* 1988;169:603-607.
 58. Gefter WB, Conant EF. Issues and controversies in the plain-film diagnosis of asbestos-related disorders in the chest. *J Thorac Imaging* 1988;3:11-28.
 59. Gefter W, Epstein D, Miller W. Radiographic evaluation of asbestos-related chest disorders. *Crit Rev Diagn Imaging* 1984;21:123-181.
 60. Kipen HM, Lillis R, Suzuki Y, et al. Pulmonary fibrosis in asbestos insulation workers with lung cancer: a radiologic and histopathologic evaluation. *Br J Ind Med* 1987;44:96-100.
 61. Blanc PD, Gamsu G. The effect of cigarette smoking on the detection of small radiographic opacities in inorganic dust diseases. *J Thorac Imaging* 1988;3:51-56.
 62. Blanc P, Golden J, Gamsu G. Asbestos exposure-cigarette smoking interactions among shipyard workers. *JAMA* 1988;259:370-373.
 63. Weiss W. Cigarette smoke, asbestos, and small irregular opacities. *Am Rev Respir Dis* 1984;130:293-301.
 64. Weiss W. Presentation of data on pulmonary fibrosis and cigarette smoking, letter. *Am J Ind Med* 1984;5:417-419.
 65. Aberle DR, Gamsu G, Ray CS. High-resolution CT of benign asbestos-related diseases: clinical and radiographic correlation. *AJR Am J Roentgenol* 1988;151:883-891.
 66. Aberle DR, Gamsu G, Ray CS, et al. Asbestos-related pleural and parenchymal fibrosis: detection with high-resolution CT. *Radiology* 1988;166:729-734.
 67. Staples CA, Gamsu G, Ray CS, et al. High-resolution computed tomography and lung function in asbestos-exposed workers with normal chest radiographs. *Am Rev Respir Dis* 1989;139:1502-1508.
 68. Bergin CJ, Castellino RA, Blank N, et al. Specificity of high-resolution CT findings in pulmonary asbestosis: do patients scanned for other indications have similar findings? *AJR Am J Roentgenol* 1994;163:551-555.
 69. al Jarad N, Strickland B, Pearson MC, et al. High-resolution computed tomographic assessment of asbestosis and cryptogenic fibrosing alveolitis: a comparative study. *Thorax* 1992;47:645-650.
 70. Friedman AC, Fiel SB, Fisher MS, et al. Asbestos-related pleural disease and asbestosis: a comparison of CT and chest radiography. *AJR Am J Roentgenol* 1988;150:269-275.
 71. Oksa P, Suoranta H, Koskinen H, et al. High-resolution computed tomography in the early detection of asbestosis. *Intl Arch Occup Environ Health* 1994;65:299-304.
 72. Neri S, Boraschi P, Antonelli A, et al. Pulmonary function, smoking habits, and high-resolution computed tomography (HRCT) early abnormalities of lung and pleural fibrosis in shipyard workers exposed to asbestos. *Am J Ind Med* 1996;30:588-595.
 73. Akira M, Yokoyama K, Yamamoto S, et al. Early asbestosis: evaluation with high-resolution CT. *Radiology* 1991;178:409-416.
 74. Akira M. Uncommon pneumoconiosis: CT and pathologic findings. *Radiology* 1995;197:403-409.
 75. Han DH, Goo JN, Im JG, et al. Thin-section CT findings of arc-welders' pneumoconiosis. *Korean J Radiol* 2000;1:79-83.
 76. Voelz GL, Lawrence JN, Johnson ER. Fifty years of plutonium exposure to the Manhattan Project plutonium workers: an update. *Health Phys* 1997;73(4):611-619.
 77. Aronchick JM, Rossman MD, Miler WT. Chronic beryllium disease: diagnosis, radiographic findings, and correlation with pulmonary function tests. *Radiology* 1987;163:677-682.
 78. International Labor Office. *Guidelines for the use of ILO international classification of radiographs of pneumoconioses*. Occupational Safety and Health Series, No. 22 (rev). Geneva, Switzerland: International Labor Office, 1980.
 79. Weber AL, Stoockle JD, Hardy HL. Roentgenologic patterns in long-standing beryllium disease: report of eight cases. *AJR Am J Roentgenol* 1965;93:879-890.
 80. Harris KM, McConnochie K, Adams H. The computed tomographic appearances in chronic berylliosis. *Clin Radiol* 1993;47:26-31.
 81. Newman LS, Buschman DL, Newell JD, et al. Beryllium disease: assessment with CT. *Radiology* 1994;190:835-840.
 82. Daniloff E, Lynch DA, Bartelson B, et al. Observer variation and relationship of computed tomography to severity of beryllium disease. *Am J Respir Crit Care Med* 1997;155:2047-2056.
 83. White CS, Templeton PA. Chemical pneumonitis. *Radiol Clin North Am* 1992;30:1231-1243.
 84. Kleinfeld M. Acute pulmonary edema of chemical origin. *Arch Environ Health* 1965;10:942-946.
 85. Conner EH, Dubois AB, Comroe JH. Acute chemical injury of the airway and lungs: experience with six cases. *Anesthesiology* 1962;23:538-547.
 86. Baar HS, Galindo J. Bronchiolitis fibrosa obliterans. *Thorax* 1966;21:209-214.
 87. Bardana EJ, Jr. Reactive airways dysfunction syndrome (RADS): guidelines for diagnosis and treatment and insight into likely prognosis. *Ann Allergy Asthma Immunol* 1999;83(6Pt2):583-586.
 88. King TE. Bronchiolitis. *Eur Respir Monograph* 2000;5:244-266.
 89. Kern DG, Kuhn C 3rd, Ely EW, et al. Flock worker's lung: broadening the spectrum of clinicopathology, narrowing the spectrum of suspected etiologies. *Chest* 2000;117(1):251-259.
 90. Kern DG, Crausman RS, Durand KT, et al. Flock worker's lung: chronic interstitial lung disease in the nylon flocking industry. *Ann Intern Med* 1998;129(4):261-272.
 91. Raymond LW. Flock worker's lung. *Ann Intern Med* 1999;130(7):615-616.
 92. Weiland DA, Lynch DA, Jensen S, et al. High-Resolution CT Findings in Flock Worker's Lung: A Newly Described Work-related Interstitial Lung Disease. *Radiology* (submitted for publication).
 93. Lynch DA, Rose CS, Way D, et al. Hypersensitivity pneumonitis: sensitivity of high-resolution CT in a population-based study. *AJR Am J Roentgenol* 1992;159:469-472.
 94. Hartley PG, Galvin JR, Hunninghake GW, et al. High-resolution CT-derived measures of lung density are valid indexes of interstitial lung disease. *J Appl Physiol* 1994;76:271-277.
 95. Lynch DA, Newell JD, Logan P, et al. Can CT distinguish idio-

- pathic pulmonary fibrosis from hypersensitivity pneumonitis? *AJR Am J Roentgenol* 1995;165:807-811.
96. Jarad NA, Wilkinson P, Pearson MC, et al. A new high resolution computed tomography scoring system for pulmonary fibrosis, pleural disease, and emphysema in patients with asbestos related disease. *Br J Ind Med* 1992;49:73-84.
97. Schaeffner ES, Miller DP, Wain JC, et al. Use of an asbestos exposure score and the presence of pleural and parenchymal abnormalities in a lung cancer case series. *Int J Occup Environ Health* 2001;7(1):14-18.
98. Harkin TJ, McGuinness G, Goldring R, et al. Differentiation of the ILO boundary chest roentgenograph (0/1 to 1/0) in asbestosis by high-resolution computed tomography scan, alveolitis, and respiratory impairment. *J Occup Envir Med* 1996;38(1):46-52.
99. Wollmer P, Jakobsson K, Albin M, et al. Measurement of lung density by X-ray computed tomography: relation to lung mechanics in workers exposed to asbestos cement. *Chest* 1987;91:865-869.
100. Reuter M, Holling I, Emde L, et al. Quantitative computed tomography of the lung in the early diagnosis of asbestosis: initial results in asbestos-exposed navy personnel. *Rofo Fortschr Geb Rontgenstr Neuen Bildgeb Verfahr* 1995;162(4):288-295.